

Journal of Visualized Experiments

Methods for Measuring the Orientation and Rotation Rate of 3D-Printed Particles in Turbulence --Manuscript Draft--

Manuscript Number:	JoVE53599R4
Full Title:	Methods for Measuring the Orientation and Rotation Rate of 3D-Printed Particles in Turbulence
Article Type:	Methods Article - JoVE Produced Video
Keywords:	Turbulence; anisotropic particles; particle tracking
Manuscript Classifications:	93.34: Fluid Mechanics and Thermodynamics; 93.34.54: multiphase flow
Corresponding Author:	Greg A Voth Wesleyan University Middletown, Connecticut UNITED STATES
Corresponding Author Secondary Information:	
Corresponding Author E-Mail:	gvoth@wesleyan.edu
Corresponding Author's Institution:	Wesleyan University
Corresponding Author's Secondary Institution:	
First Author:	Brendan Cole
First Author Secondary Information:	
Other Authors:	Brendan Cole Guy G Marcus Stefan Kramel Shima Parsa Rui Ni
Order of Authors Secondary Information:	
Abstract:	Experimental methods are presented for measuring the rotational and translational motion of anisotropic particles in turbulent fluid flows that allow for analysis of particles of any shape that can be modeled on a computer using multiple slender rods. 3D printing technology is used to fabricate particles with slender arms connected at a common center. We describe experimental methods for measuring the rotational and translational motion of anisotropic particles in turbulent fluid flows. We use 3D printing technology to fabricate particles with slender arms connected at a center. Shapes explored include crosses (two perpendicular rods), jacks (three perpendicular rods), triads (three rods in a plane symmetric about a common end point), and tetrads (four arms with tetrahedral symmetry). Methods for producing on the order of 10,000 fluorescently dyed particles are described. Time-resolved measurements of their orientation and solid-body rotation rate are obtained from four video images of their motion in a turbulent flow between oscillating grids with $R_\lambda = 91$. In this relatively low Reynolds number flow, the advected particles are small enough that they approximate anisotropic ellipsoidal tracer particles. We present results of time-resolved 3D trajectories of position and orientation of the particles as well as measurements of their rotation rates as well as measurements of their rotation rate and preferential alignment.
Author Comments:	We have tried to take the editors comments into account. We believe that the results figures that were previously published in New Journal of Physics do not need permission for reproduction: http://iopscience.iop.org/1367-

	2630/page/NJP%20copyright%20statement
Additional Information:	
Question	Response
If this article needs to be filmed by a certain date to due to author/equipment/lab availability, please indicate the date below and explain in your cover letter.	
If this article needs to be "in-press" by a certain date to satisfy grant requirements, please indicate the date below and explain in your cover letter.	

TITLE:

Methods for Measuring the Orientation and Rotation Rate of 3D-Printed Particles in Turbulence

AUTHORS:

Cole, Brendan C.

Department of Physics

Wesleyan University

Middletown, CT, USA

bcole@wesleyan.edu

Marcus, Guy G.

Department of Physics

Wesleyan University

Middletown, CT, USA

guygmarcus@jhu.edu

Parsa, Shima

Department of Physics

Wesleyan University

Middletown, CT, USA

sparsa@seas.harvard.edu

Kramel, Stefan

Department of Physics

Wesleyan University

Middletown, CT, USA

skramel@wesleyan.edu

Ni, Rui

Department of Physics

Wesleyan University

Middletown, CT, USA

ruiniphy@gmail.com

Voth, Greg A.

Department of Physics

Wesleyan University

Middletown, CT, USA

gvoth@wesleyan.edu

CORRESPONDING AUTHOR:

Greg Voth

KEYWORDS:

particles in turbulence, anisotropic particles, turbulence, 3D printing, rotation, fluid dynamics

SHORT ABSTRACT:

We use 3D printing to fabricate anisotropic particles in the shapes of jacks, crosses, tetrads, and triads, whose alignments and rotations in turbulent fluid flow can be measured from multiple simultaneous video images.

LONG ABSTRACT:

Experimental methods are presented for measuring the rotational and translational motion of anisotropic particles in turbulent fluid flows. 3D printing technology is used to fabricate particles with slender arms connected at a common center. Shapes explored are crosses (two perpendicular rods), jacks (three perpendicular rods), triads (three rods in triangular planar symmetry), and tetrads (four arms in tetrahedral symmetry). Methods for producing on the order of 10,000 fluorescently dyed particles are described. Time-resolved measurements of their orientation and solid-body rotation rate are obtained from four synchronized videos of their motion in a turbulent flow between oscillating grids with $R_\lambda = 91$. In this relatively low-Reynolds number flow, the advected particles are small enough that they approximate ellipsoidal tracer particles. We present results of time-resolved 3D trajectories of position and orientation of the particles as well as measurements of their rotation rates.

INTRODUCTION:

In a recent publication, we introduced the use of particles made from multiple slender arms for measuring rotational motion of particles in turbulence¹. These particles can be fabricated using 3D printers, and it is possible to accurately measure their position, orientation, and rotation rate using multiple cameras. Using tools from slender body theory, it can be shown that these particles have corresponding effective ellipsoids², and the rotational motions of these particles are identical to those of their respective effective ellipsoids. Particles with symmetric arms of equal length rotate like spheres. One such particle is a jack, which has three mutually perpendicular arms attached at its center. Adjusting the relative lengths of the arms of a jack can form a particle equivalent to any tri-axial ellipsoid. If the length of one arm is set equal to zero, this creates a cross, whose equivalent ellipsoid is a disk. Particles made of slender arms take up a small fraction of the solid volume of their solid ellipsoidal counterparts. As a result, they sediment more slowly, making them easier to density match. This allows the study of much larger particles than is convenient with solid ellipsoidal particles. Additionally, imaging can be performed at much higher particle concentrations because the particles block a smaller fraction of the light from other particles.

In this paper, methods for fabrication and tracking of 3D-printed particles are documented. Tools for tracking the translational motion of spherical particles from particle positions as seen by multiple cameras have been developed by several groups^{3,4}. Parsa *et al*⁵ extended this approach to track rods using the position and orientation of the rods seen by multiple cameras. Here, we present methods for fabricating particles of a wide variety of shapes and reconstructing their 3D orientations. This offers the possibility to extend 3D tracking of particles with complex shapes to a wide range of new applications.

This technique has great potential for further development because of the wide range of particle shapes that can be designed. Many of these shapes have direct applications in environmental

flows, where plankton, seeds, and ice crystals come in a vast array of shapes. Connections between particle rotations and fundamental small-scale properties of turbulent flows⁶ suggest that study of rotations of these particles provides new ways to look at the turbulent cascade process.

PROTOCOL:

1. Fabrication of Particles

1.1. Use a 3D Computer Aided Drafting program to create particle models. Export one file per model in a file format that can be processed by the 3D printer used.

1.1.1. Use the Circle command to draw a circle with a diameter of .3 mm. Use the Extrude function to make a cylinder with a length of 3 mm.

1.1.2. Make a cross with two orthogonal cylinders with a common center; make a jack with three mutually orthogonal cylinders with a common center; make a tetrad with four cylinders sharing a common end at 109.5° angles to one another; make a triad with three cylinders in a plane sharing a common end at 120° angles to one another.

1.1.3. To tilt cylinders (hereafter called “arms” of the particles) with respect to one another, use the Rotate 3D command to draw a line across the diameter of the circle at one of its ends and then enter the desired angle of rotation.

1.1.4. Use the Union command to join the different arms together into a single watertight object.

1.1.5. Use Rotate 3D again to tilt the object so that no arms are along the vertical or horizontal axes, because arms that lie along these axes tend to have defects, break off more easily, or flatten out.

1.1.6. Export each object in a separate file in a format that can be used by 3D printers.

1.2. Order approximately 10,000 particles of each type from a commercial source that specializes in additive manufacturing or print them at an available facility. Particles should be printed on a polymer extrusion printer that uses a support matrix of a different material that can be dissolved away.

1.2.1. Order the particles three weeks or more before experiments are planned because the arrangement and printing of so many particles is a slow process. Ensure that particles are printed on “high-resolution mode” because the particles are near the minimum feature size of many 3D printers and the arms will not be as symmetric and may break if printed at lower resolution.

2. Preparation of Particles

2.1. Prepare a salt solution in which the particles are neutrally buoyant to minimize particles’ arms bending while in storage and so that gravitational and buoyancy forces do not have to be

accounted for in the analysis.

2.1.1. Test average particle densities by immersing particles in solutions of water mixed with calcium chloride (CaCl_2) at densities around 1.20 g/cm^3 .

2.1.1.1. To determine water density, first zero a scale while an empty 100 mL volumetric flask is on top of it. Take the flask off and fill it with water mixed with CaCl_2 . Place the flask back atop the scale and divide the given mass by 100 mL.

Note: Because $1 \text{ mL} = 1 \text{ cm}^3$, $1 \text{ g/mL} = 1 \text{ g/cm}^3$.

2.1.1.2. Test particles at many different solution densities, ranging from 1.16 g/cm^3 to 1.25 g/cm^3 , in roughly 0.01 g/cm^3 increments. Test multiple particles at every density because not all particles will have the same density: in the same solution, some will sink, some will be neutrally buoyant, and some will float.

2.1.2. Record at which density particles are, on average, neutrally buoyant after several hours.

Note: The density found may be significantly different from the bulk density quoted by the particle manufacturers.

2.1.3. Mix about 400 kg of CaCl_2 into approximately 1600 L of water until the solution is at the density recorded in 2.1.1 – 2.1.2.

2.1.4. Remove about 1 L of this mixed solution per particle type (jacks, tetrads, etc.) to be used for storage of particles. Hold each liter in a different container at room temperature. Store the remainder of the solution at room temperature in a large storage tank.

[Place Figure 1 here]

2.2. Manually loosen the support material in which the particles come encased by gently breaking the large pieces (~ $5 \times 320 \text{ mm}$, part of which is shown in Figure 1a) into small sections (~ $5 \times 5 \text{ mm}$, Figure 1b), then manually massage each section until much of the excess resin has come off (Figure 1c-e). Remove excess resin in this way to reduce the amount of the NaOH solution that will need to be created for steps 2.2.1 – 2.2.4.

2.2.1. Place the remaining resin block in a 10% by mass sodium hydroxide (NaOH) solution immersed in an ultrasonic bath for one hour. The resin is a different material than the particles are, so the NaOH will remove the resin without permanently affecting the particles.

CAREFUL: The solution is corrosive and will get hot while in the ultrasonic bath.

2.2.2. Filter out particles.

2.2.2.1. To filter particles, create a funnel using netting with $.1016 \times .13462 \text{ cm}$ plastic holes. Hold the funnel over the container to be used for the disposal of the NaOH solution and slowly

pour the solution through. Dispose of NaOH solution in accordance with environmental health and safety guidelines.

2.2.3. Rinse particles gently with water before immersing in a new 10% by mass NaOH solution in an ultrasonic bath for another half hour.

2.2.4. Filter out particles as in 2.2.2.1 and store in the density-matched solution separated in 2.1.4 while they harden. Handle the particles carefully because the NaOH solution temporarily softens them.

Note: If particles are not stored in a density-matched solution, some arms may bend. Keeping them immersed in the density-matched solution for several hours also allows some voids in the plastic to fill with fluid.

2.3. Dye particles with Rhodamine-B mixed with water so that they fluoresce under the light emitted by a green laser.

2.3.1. Prepare a 1 L solution of Rhodamine-B dye in water at a concentration of .5 g/L (afterward referred to as “dye”).

CAUTION: Toxic.

2.3.2. Heat the dye to a temperature between 50 and 80 °C, depending on particle material. Use higher temperatures for harder plastics; using too high of a temperature will result in the arms bending.

2.3.3. Put ~2,500 particles, enough to loosely fill ~25 mL in the density-matched storage solution, in the dye and keep all at 80 °C for two to three hours to allow the dye to absorb into the polymer. Remove particles once they are pink, like the one in Figure 1f.

CAREFUL: The heat will soften the particles temporarily.

2.3.4. Filter out particles and rinse them under a faucet before storage in the designated solutions separated in 2.1.4. The particles will lose a small fraction of their dye, making the solution pink, but rinsing under the faucet helps prevent losing a detrimental amount of dye..

Note: Average particle density will have changed due to dyeing, so test again as in 2.1.1–2.1.2 to find the new solution density at which particles are, on average, neutrally buoyant.

2.4. Change bulk CaCl₂ solution (from 2.1.3) density as needed. Repeat 2.1.4 and remove new volumes of density-matched solution. Dispose of former storage solutions, which will now have small amounts of Rhodamine-B dye in them, in accordance with environmental health and safety regulations.

2.5. Repeat 2.3.2–2.3.4 for successive sets of ~2500 particles, storing all particles of the same shape in the same density-matched solutions created in 2.4, separated from particles of different

shapes.

Note: After about 5 repetitions of 2.3.2–2.3.4, the Rhodamine-B solution will no longer be a high enough concentration to effectively dye particles.

2.6. Dispose of the solution created in 2.3.1 in accordance with environmental health and safety regulations, then repeat 2.3.1 and create a new .5g/L solution with which to dye particles.

2.7. Repeat 2.6 every 5 repetitions of 2.3.2–2.3.4.

3. Experimental and Optical Setup

[Place Figure 2 Here]

3.1. Prepare the cameras.

3.1.1. Use cameras capable of at least 1 megapixel resolution at 450 frames per second.

3.1.2. Arrange the cameras such that each camera is pointing at, and is focused on, the center of the viewing volume. Fewer cameras can be used, however shadowing of an arm of a particle by another arm limits the orientation measurement accuracy, and having fewer cameras makes experiments more susceptible to this effect. Using more than four cameras could likewise increase orientation measurement precision because it will reduce the chance of arms being shadowed on all cameras, which is a primary source of uncertainty.

3.1.3. Position the cameras with large ($\sim 90^\circ$) angles between each pair subject to constraints of the apparatus. Place cameras as shown in Figure 2 to balance experimental access and the size of the angle between individual cameras. Minimize optical distortions by building viewing ports into the apparatus perpendicular to each camera viewing direction.

3.1.4. Use 200 mm macro lenses on each camera to obtain the desired measurement volume from a working distance of half a meter. The volume viewed by all four cameras determines the detection volume, which is about $3 \times 3 \times 3 \text{ cm}^3$.

3.1.5. Calibrate the cameras to allow transformation from measured pixel positions to coordinates in 3D space.

3.1.5.1. Set the apertures to f/11 and mount 532 nm notch filters to remove laser light while allowing through longer-wavelength fluorescence onto the cameras

3.1.5.2. Place an image calibration mask in the tank, fill the tank with the bulk solution from 2.4, and illuminate the mask.

3.1.5.3. Adjust the cameras so they each have the mask in view and they all are focused on the same point on the mask. Carefully align the cameras to optimize the shape of the detection volume.

3.1.5.4. Be careful to change as little as possible about the optical setup from this point forward.

3.1.5.5. Acquire and store images of the mask from each camera.

3.1.5.6. Drain the solution out of the tank and pump it back where it had previously been stored.

3.1.5.7. Extract the parameters specifying the position, viewing direction, magnification, and optical distortions of each camera from the calibration images. Do this by identifying places on the calibration mask visible on all four cameras and defining the distance between these points. With this information, use standard calibration methods to extract relevant parameters.

Note: The basic calibration method is described in Tsai, 1987⁷. The implementation used in these experiments is described in Oullette *et al*³. Researchers wishing to develop camera calibration software may also want to consider OpenPTV⁴.

3.1.5.8. Create a final calibration file using a dynamic calibration process. This is done after tracer particle data has been acquired. Use a nonlinear least squares search to optimize the camera calibration parameters and obtain the smallest mismatch between the positions of particles seen on multiple cameras. These methods are described in Ref. ⁸ and ⁹.

3.2. With a Q-switched green Nd:YAG laser capable of 50 W average power (hereafter called the “laser”), illuminate a cylinder in the center of the tank with roughly a 3 cm cross-sectional diameter, where the flow is homogeneous.⁸

Note: The laser power is specified at a pulse frequency of 5 kHz. The pulse frequency in these experiments is 900 Hz, where the output power is significantly lower.

3.2.1. Split the light from the laser using a beam splitter and use mirrors to guide one beam into the front of the tank and the other, orthogonal to the first, into the side of the tank.

3.2.2. Place two additional mirrors outside of the tank, opposite where the beams are entering, in order to reflect light back into the tank and create more uniform illumination, dramatically decreasing shadowing effects.

Note: The length scale of interference effects from the counter-propagating beams is too small to significantly affect these experiments.

4. **Perform the Experiments**

4.1. Prepare to record video from each camera.

4.1.1. Program an image compression system that removes unwanted image data in real time.^{10,13}

4.1.1.1. If the camera does not have a particle in view, do not save the image.

4.1.1.2. Where there are bright pixels, save only the location and brightness of bright pixels instead of the whole image.

Note: Because each particle typically covers approximately 5,000 bright pixels and there is rarely more than one particle in view at a time, the image compression system dramatically reduces the amount of storage required to record with high-speed cameras for many hours.

4.1.2. Prepare the data acquisition software.

4.2. Prepare the turbulent flow in a $1 \times 1 \times 1 \text{ m}^3$ octagonal tank using two parallel 8 cm mesh grids oscillating in phase. **Error! Bookmark not defined.**

4.2.1. Pump the CaCl_2 solution from 2.4 into a vacuum chamber and keep it in the chamber overnight to degas the solution, which minimizes air bubbles in the experiments.

4.2.2. Pump solution from the vacuum chamber through a $0.2 \mu\text{m}$ filter into the octagonal tank where experiments will be performed.

4.3. Run the experiment.

4.4. Choose one particle type (tracer particles, jacks, crosses, tetrads, or triads) to be used for the first round of experiments and add all 10,000 of those particles into the water through a port at the top of the apparatus. Close this port after adding particles.

4.4.1. Turn the laser on.

4.4.2. Set cameras and laser to respond to an external trigger and set the frequency of the trigger to 450 Hz for the cameras and 900 Hz for the laser. Use the external trigger to ensure all cameras start acquisition simultaneously and remain synchronized throughout the recording

4.4.3. Open the laser aperture.

4.4.4. Set the grid to the chosen frequency (1 or 3 Hz) and start it running. Before starting data acquisition, run the grid for about 1 minute to allow turbulence to fully develop.

4.4.5. Record 10^6 frames in order to keep the file size manageable and to keep any errors that may occur in the image compression systems from compromising too much data.

4.4.6. Close the laser aperture and stop the camera trigger. Reset the image compression systems and the cameras.

4.4.6.1. Check that the video files are not corrupted by viewing portions of each file.

4.4.7. Repeat 4.4.1 – 4.4.6 until 10^7 images have been recorded at the chosen grid frequency for the chosen particle.

4.5. Change the grid frequency to the one not chosen in 4.4.4 and repeat 4.4.4 – 4.4.7

4.6. Empty the tank and filter the water to remove all particles. Save particles in the storage water from 2.4 if desired.

4.7. Repeat 4.4 – 4.6 for all particle types.

4.8. After all experiments have been finished, calibrate cameras once more, as in 3.1.5–3.1.5.7.

5. Data Analysis

Note: This section of the Protocol presents an overview of the process used to obtain particle orientations and rotation rates. The specific programs used, along with test images and calibration files, are included as a supplement to this publication, and are open to use by any interested readers.

5.1. Using the camera calibration parameters, obtain the 3D position and orientation from images of particles on multiple cameras.

5.1.1. At every frame, find the center of the particle on each of the four images. All particles in these experiments are sufficiently symmetric that the center of the object is at the geometric center of the bright pixels on the image when viewed from any perspective.

5.1.2. Find the 3D position of the particle by stereomatching its simultaneous 2D positions on all four cameras³**Error! Bookmark not defined..**

5.1.3. Create a numerical model of the particle that can be projected onto each camera to model the intensity in the image from that camera.

5.1.3.1. Model the particle as a composite of rods. Using the camera calibration parameters from 3.1.5.7 and 3.1.5.8, project the two end points of each rod onto the cameras and then model the distribution of light intensity in two dimensions, with a Gaussian function across the width of the rod and a Fermi-Dirac function across its length according to software protocol.

5.1.3.2. Model light intensity in two dimensions in this way to minimize the computational cost of the data analysis. Projection of a full three-dimensional model of the fluorescent particle could improve on this approach, but would be much more computationally intensive.

5.1.3.3. Click Run to begin analysis.

5.1.4. Choose an initial guess of the particle orientation.

5.1.4.1. If analyzing the first frame in which this particle is visible, the first guess can be a random set of Euler angles.

5.1.4.2. If this particle was in at least one previous frame, use the orientation found using the previous frame as the initial guess.

5.1.5. Perform a nonlinear least-squares fit to determine the particle orientation.

5.1.5.1. Optimize the three 3D position coordinates and the three Euler angles such that the squared difference between the measured intensity and the 2D projection of the model is minimized on all four cameras according to software protocol.

Note: There are multiple conventions for defining Euler angles. Define the angles, (φ, θ, ψ) , as follows: φ is an initial rotation about the z axis, creating new axes x' and y' ; θ is a rotation about x' , creating new axes z' and y'' ; ψ is a rotation about the new z' axis.¹¹

5.1.6. Choose the orientation that requires the smallest rotation with respect to the previous frame. For a jack, the Euler angles found give one of the 24 symmetric orientations; for a tetrad it is one of 12 symmetric orientations; for a cross, it is one of 8 symmetric orientations; and for a triad it is one of 6 symmetric orientations.

Note: The method in 5.1.6 assumes that the particle will not rotate more than half of one of its interior angles between frames. Justification for this assumption is given in the Discussion.

5.2. Save the position and Euler angles as a function of time.

5.3. Use these data to extract solid-body rotation rate and other quantities.

REPRESENTATIVE RESULTS:

Figure 3a shows an image of a tetrad from one of our cameras above a plot of the Euler angles obtained from a section of its trajectory (Figure 3c). In Figure 3b, the results of the orientation-finding algorithm, described in Protocol 5 – 5.3, are superimposed on the tetrad image. The arms of the tetrad in Figure 3a do not follow the simple intensity distributions that are used to create the model (Protocol 5.1.3.1). This is true for all of the particles. The observed intensity furthermore has a non-trivial dependence on the angles between the arms, the illumination, and the viewing direction¹². The models do not include any of these factors but nonetheless produce very accurate measurements of particle orientations.

Once an orientation is found with a least-squares fit, the 3D coordinates of the particle center and the three Euler angles, (φ, θ, ψ) , that specify its orientation matrix¹¹ are saved. This is done for every frame where the particle is in view of all four cameras. These data enable the reconstruction of the complete trajectory of the particle across the viewing volume, as are shown in Figure 4 for a cross and a jack. Figure 4 was made using the Paraview open source visualization package and is based on measurements made with images from the experiments.

[Place Figure 3 Here]

[Place Figure 4 Here]

Two different but related quantities based on particle orientations are calculated over the entire trajectory: tumbling rate and solid-body rotation rate. Tumbling rate, $\dot{\mathbf{p}}$, is the rate of change of the unit vector defining the orientation of the particle. In previous measurements of rods, \mathbf{p} was defined as the axis of symmetry along the rod; for crosses and triads, \mathbf{p} is normal to the plane of the arms; for jacks and tetrads, \mathbf{p} is along one of the arms. Because rotation along the axis of rods cannot be directly measured, studies of the rotations of rods in turbulence have largely been limited to measuring the tumbling rate. This is not an issue for any of the particles in these experiments. All rotations of these particles can be measured and, with orientation measurements smoothed along a particle's trajectory, the full solid-body rotation rate vector, $\boldsymbol{\omega}_s$, can be found.

To extract the solid-body rotation rate from measured particles orientations, smoothing needs to be done over several time steps. The problem is to find the rotation matrix \mathbb{R} that relates an initial orientation $\mathbb{O}(t_i)$ to the measured orientations $\mathbb{O}(t)$ at a sequence of time steps:

$$\mathbb{O}(t) = \mathbb{R}^{\frac{t-t_i}{\tau_f}} \mathbb{O}(t_i),$$

where τ_f is the period between images and t_i is the time of the initial frame. In Marcus *et al*¹, we used a nonlinear least-squares fit to determine the six Euler angles defining the initial orientation matrix, $\mathbb{O}(t_i)$, and the rotation matrix over a single time step, \mathbb{R} , that best match the measured orientation matrices as a function of time. More recent work has shown that this algorithm sometimes has difficulty when the rotation rate is small because the nonlinear search is exploring the region where the Euler angles are approximately equal to zero and are degenerate. In the case where the rotation in a time step is sufficiently small, \mathbb{R} can be linearized using $\mathbb{R}^{(t-t_i)/\tau_f} = \boldsymbol{\Omega}(t - t_i)$, where $\boldsymbol{\Omega}$ is a rotation rate matrix. As described in the Discussion below, these experiments are in this low rotation limit, so $\boldsymbol{\Omega}$ can be found from the measured $\mathbb{O}(t)$ using a linear least squares fit.

From the measured rotation matrix over a time step, \mathbb{R} , we can extract the solid-body rotation rate and the tumbling rate. By Euler's theorem¹¹ \mathbb{R} can be decomposed as a rotation by an angle Φ about the solid-body rotation axis, $\hat{\boldsymbol{\omega}}_s$. The magnitude of the solid-body rotation rate is $\omega_s = \Phi/\tau_f$. The tumbling rate is the component of the solid-body rotation rate perpendicular to the orientation of the particle, and so it can be calculated as $\dot{\mathbf{p}} = \boldsymbol{\omega}_s \times \mathbf{p}$. Figure 5 compares PDFs of the measured mean square tumbling rate for crosses and jacks to direct numerical simulations of spheres. Small jacks rotate just like spheres in fluid flows¹, so the fact that the PDF for jacks agrees with the simulated PDF for spheres demonstrates that the experiments are able to capture the rare high rotation events that occur in turbulent flows.

[Place Figure 5 Here]

Figure 1: A jack at various stages of resin removal. a) The blocks of support resin that the particles arrive in. b) A single block separated from the rest. c-e) Multiple stages of resin removal done by hand. f) A single jack after the NaOH bath.

Figure 2: Experimental setup. In the octagonal flow between oscillating grids, a central viewing volume in the focus of the four video cameras is illuminated by a green Nd:YAG laser. a) Side view showing how the four cameras are arranged and connected to computers. Figure from ¹³. b) Top view showing laser, mirror, and lens configuration to achieve uniform illumination in the

central volume.

Figure 3: **Reconstructed particle orientations from measured images.** a) A sample image from one of the four cameras. The object shown is a tetrad, which has four arms at 109.5° interior angles to one another. b) The same tetrad shown with the results of our orientation-finding algorithm. c) Measured Euler angles plotted as a function of time for a single trajectory.

Figure 4: **Reconstructed trajectories of a cross (a) and a jack (b) in three-dimensional turbulence.** (a) The two different color sheets trace the path of the two arms of the particle through space over time. The length of the track is 336 frames, or $5.7 \tau_\eta$, and a cross is shown every 15 frames. (b) The blue, orange, and blue-green paths trace the paths of the three arms of the jack as the particle rotates and moves through the fluid. The dark green line denotes the path of the jack's center. The length of the particle track is 1025 frames, or $17.5 \tau_\eta$, and a jack is shown every 50 frames. (*Note: Neither the crosses nor the jacks above are drawn to scale.*). Figure from ¹, where it is Figure 3.

Figure 5: **PDF of mean-square tumbling rate.** The probability density function of the measured mean-square tumbling rate for our crosses (red squares) and jacks (blue circles) as well as direct numerical simulations of spheres (solid line). Error bars include the random error due to limited statistical sampling estimated by dividing the data set into subsets, as well as the systematic error that results from the fit length dependence of the tumbling rate, which is estimated by performing the analysis at a range of fit lengths. Figure from ¹ where it is Figure 5.

DISCUSSION:

Measurements of the vorticity and rotation of particles in turbulent fluid flow have long been recognized as important goals in experimental fluid mechanics. The solid-body rotation of small spheres in turbulence is equal to half the fluid vorticity, but the rotational symmetry of spheres has made direct measurement of their solid-body rotation difficult. Traditionally, the fluid vorticity has been measured using complex, multi-sensor, hot-wire probes¹⁴. But these sensors only get single-point vorticity measurements in airflows that have large mean velocity. Other vorticity measurement methods have been developed. For example, Su and Dahm used flow field velocimetry based on scalar images¹⁵ and Lüthi, Tsinober, and Kinzelbach used 3D particle tracking velocimetry¹⁶. Measurements of vorticity in turbulence by tracking rotations of single particles were pioneered by Frish and Webb, who measured the rotations of solid spherical particles using a vorticity optical probe¹⁷. This probe uses small particles with planar crystals embedded that act as mirrors to create a beam whose direction changes as the particle rotates. Recently, methods have been developed for measuring the rotational motion of large spherical particles using imaging of patterns painted on the particles^{18,19} or fluorescent particles embedded in transparent hydrogel particles²⁰. To track anisotropic particles, Bellani *et al.* have used custom-molded hydrogel particles²¹. Parsa *et al.* have tracked the rotations of segments of nylon threads^{5,6,12}. The methods for measuring vorticity and particle rotations presented in this paper have advantages over these alternative methods. 3D-printed anisotropic particles can be small, with arm thicknesses down to .3 mm in diameter, and their rotations can still be resolved very accurately. Other methods traditionally require larger particles because they involve the resolution of structures on or within the particles themselves. In addition, the use of image compression systems allows for many more particle trajectories to be recorded and measured

than would otherwise be reasonable. Having more measurements makes it possible to study rare events like those with very high rotation rates in Figure 5, which reveal intermittency phenomena of great interest to researchers.

Particle concentrations in these experiments were about $5 \times 10^{-3} \text{ cm}^{-3}$, which meant that typically only about 20% of images from the cameras had a particle. To study rare events, thousands of particle trajectories are typically required, which meant that hundreds of thousands of images of particles were needed. With these low concentrations, therefore, millions of images needed to be recorded to obtain an adequate volume of data. If real-time image compression systems were not used to facilitate data acquisition, this would require hundreds of TB of data storage and the analysis would be much more computationally intensive. Image compression systems decrease this load by factors of several hundred¹⁰. However, standard video recording would be adequate for higher particle densities and if data storage space is not an issue. If 100,000 particles of each type were ordered instead of 10,000, fewer images would, in principle, be needed to capture the same statistics. However, at higher particle densities particles begin to shadow one another more often. That is, there will be more times when there are particles between the laser and the particle in view, or between the particle in view and the camera. These shadowing events make measuring orientations throughout a track across the viewing volume more difficult and less reliable. For these reasons, lower particle concentrations were chosen for these experiments and image compression systems were therefore necessary.

There may be times when arm shadowing will affect the results of the nonlinear search algorithm. For certain orientations of the jack, arm shadowing causes there to be multiple minima in Euler angle space, which lead to indeterminacies in the measured orientations. This reduces the accuracy of orientation measurements for these particular orientations and occasionally leads to erroneously high measurements of the solid-body rotation rate, which pushes additional probability density towards the tail of the PDF in Figure 5. For jacks, whose arms are perpendicular to each other, this issue could be decreased by changing the angles of the cameras with respect to one another to be farther away from 90° . If the configuration of the apparatus makes this change difficult to implement, one alternative is to change the geometry of the particles to decrease shadowing. This was the reason tetrads were chosen for experiments after those with jacks had been completed, and recent tetrad measurements have shown significantly improved orientation accuracy when compared to jacks.

The methods of 3D particle tracking presented here are not confined to this particular flow or the particle sizes and shapes we use. We have already begun experiments tracking tetrads and triads with much larger sizes using similar techniques. The use of high-speed cameras to measure particle orientations and rotations can be extended to a wide array of shapes and can be used for inertial particles as well as in the neutrally buoyant case presented here. Using more cameras would allow for an even wider array of potential particle shapes, as the primary limitations to this method are the resolution of the cameras and particles' self-shadowing, as discussed in the previous paragraph.

In step 5.1.6 of the Protocol, we smooth Euler angles measurements by assuming that a particle has not rotated by more than half of one of the interior angles between arms over the course of two frames – that is, we assume that the accurate orientation measurement at frame $i+1$ retains

the chosen symmetric orientation found for frame i . If the particle had rotated by more than half of one of these interior angles, then smoothing in this way would result in a sudden and incorrect reversal of the direction of rotation. In Ref. ⁵ we show that an upper limit on particle tumbling rate is

$$\frac{\langle \dot{p}_i \dot{p}_i \rangle}{\langle \varepsilon \rangle / \nu} = \frac{1}{6} + \frac{1}{10} \left(\frac{\alpha^2 - 1}{\alpha^2 + 1} \right)^2.$$

So the largest tumbling rate ($\alpha = 0$ or ∞) is $\langle \dot{p}_i \dot{p}_i \rangle = \frac{4}{15\tau_\eta^2}$ which for $\tau_\eta = (\langle \varepsilon \rangle / \nu)^{1/2} = .128$ s is 16.2 s^{-2} . This is a root mean square (RMS) tumbling rate of 4.0 s^{-1} . Since we record images at 450 frames per second, particles would then typically rotate 0.009 radians between frames. The smallest interior angle of any of the particles in these experiments was $\frac{\pi}{2}$, so this smoothing method would fail if particles tumble more than $\frac{\pi}{4} \approx .785$ radians between frames. Thus, we can accurately track particles with tumbling rates of more than 80 times the RMS, which is much faster than the $\sqrt{40} = 6.3$ times the RMS that we actually observe in Figure 5.

ACKNOWLEDGEMENTS:

We thank Susantha Wijesinghe who designed and constructed the image compression system we use. We acknowledge support from the NSF grant DMR-1208990.

DISCLOSURES:

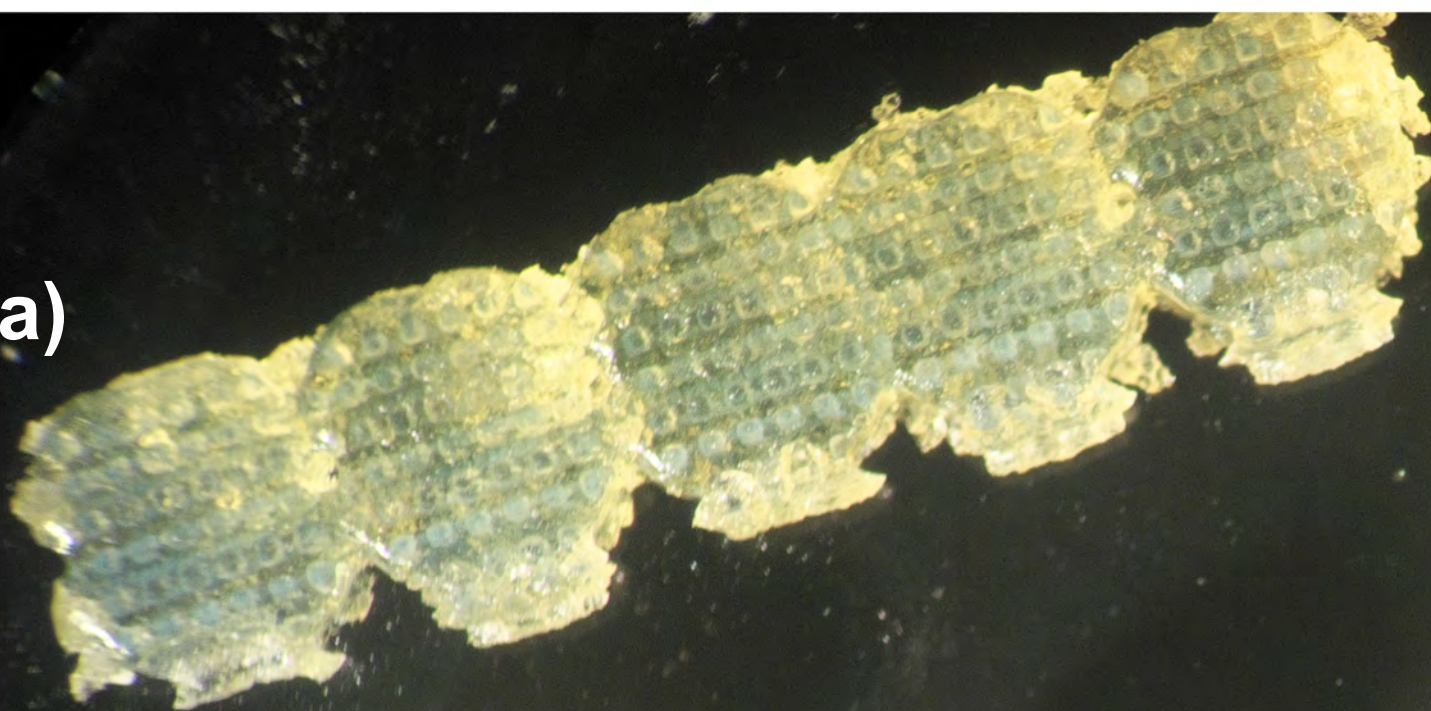
The authors have no competing financial interests to disclose.

REFERENCES:

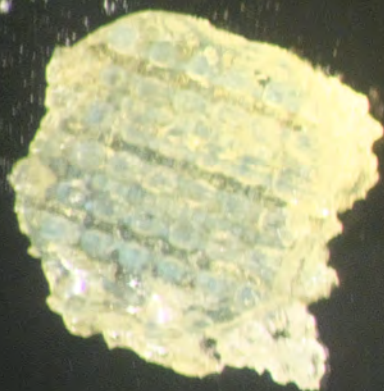
- ¹ Marcus, G., Parsa S., Kramel, S., Ni, R., and Voth, G. Measurements of the Solid-body Rotation of Anisotropic Particles in 3D Turbulence. *New J. Phys.* **16**, 102001, doi:10.1088/1367-2630/16/10/102001 (2014).
- ² Bretherton, F. The motion of rigid particles in a shear flow at low Reynolds number. *J. Fluid Mech.* **14** (02), 284-204, doi:10.1017/S002211206200124X (1962).
- ³ Oullette, N., Xu, H., Bodenschatz, E. A quantitative study of three-dimensional Lagrangian particle tracking algorithms. *Exp. in Fluids.* **40**(2), 301-313, doi: 10.1007/s00348-005-0068-7 (2006).
- ⁴ Open PTV Consortium. Open Source Particle Tracking Velocimetry. www.openptv.net (2014).
- ⁵ Parsa, S., Calzavarini, E., Toschi, F., Voth, G. Rotation Rate of Rods in Turbulent Fluid. *Phys. Rev. Lett.* **109**(13), 134501, doi: 10.1103/PhysRevLett.109.134501 (2012).
- ⁶ Parsa, S., Voth, G. Inertial Range Scaling in Rotations of Long Rods in Turbulence. *Phys. Rev. Lett.* **112** (2), 024501, doi: 10.1103/PhysRevLett.112.024501 (2014).
- ⁷ Tsai, R. A versatile camera calibration technique for high-accuracy 3d machine vision metrology using off-the-shelf tv cameras and lenses. *IEEE Journal of Robotics and Automation.* **3**(4), 323-344, doi: 10.1109/JRA.1987.1087109 (1987).
- ⁸ Blum, D., Kunwar, S., Johnson, J., Voth, G. Effects of nonuniversal large scales on conditional structure functions in turbulence. *Phys. Fluids*, **22**(1), 015107, doi: 10.1063/1.3292010 (2010).
- ⁹ J. Mann, S. Ott, and J. S. Andersen, Experimental study of relative, turbulent diffusion, *RISO Internal Report R-1036*, (1999).

-
- ¹⁰ Chan, K., Stich, D., Voth, G. Real-time image compression for high-speed particle tracking. *Rev. Sci. Instrum.*, **78**(2), 023704, doi: 10.1063/1.2536719 (2007).
- ¹¹ Goldstein, H., Poole, C., Safko, J. *Classical Mechanics*, 3rd Edition. Addison-Wesley Publishing Company, 134-180 (2002).
- ¹² Parsa, S. Rotational dynamics of rod particles in fluid flows. *Ph.D. Thesis* (Wesleyan University), (2013).
- ¹³ Wijesinghe, S. Measurement of the effects of large scale anisotropy on the small scales of turbulence. *Ph.D. Thesis* (Wesleyan University), (2012).
- ¹⁴ Wallace, J., Foss, J. The Measurement of Vorticity in Turbulent Flows. *Annu. Rev. Fluid Mech.* **27**, 469-514, doi: 10.1146/annurev.fl.27.010195.002345 (1995).
- ¹⁵ Su, L., Dahm, W. Scalar imaging velocimetry measurements of the velocity gradient tensor field in turbulent flows. I. Assessment of errors. *Phys. Fluids*. **8**, 1869-1882, doi: 10.1063/1.866970 (1996).
- ¹⁶ Lüthi, B., Tsinober, A., Kinzelbach, W. Lagrangian measurement of vorticity dynamics in turbulent flow. *J. Fluid Mech.* **528**, 87-118, doi: 10.1017/S002211200400328 (2005).
- ¹⁷ Frish, M., Webb, W. Direct measurement of vorticity by optical probe. *J. Fluid Mech.* **107**, 173-200, doi: 10.1017/S0022112081001729 (1981).
- ¹⁸ Zimmerman, R., *et al.* Tracking the dynamics of translation and absolute orientation of a sphere in a turbulent flow. *Rev. Sci. Instrum.* **82**(3), 033906, doi: 10.1063/1.3554304 (2011).
- ¹⁹ Zimmerman, R., *et al.* Rotational Intermittency and Turbulence Induced Lift Experienced by Large Particles in a Turbulent Flow. *Phys. Rev. Lett.* **106**(15), 154501, doi: 10.1103/PhysRevLett.106.154501 (2011).
- ²⁰ Klein, S., Gibert, Mathieu, Bérut, A., Bodenschatz, E. Simultaneous 3D measurement of the translation and rotation of finite-size particles and the flow field in a fully developed turbulent water flow. *Meas. Sci. Technol.* **24**(2), 1-10, doi: 10.1088/0957-0233/24/2/024006 (2013).
- ²¹ Bellani, G., Byron, M., Collignon, A., Meyer, C., Variano, E. Shape effects on turbulent modulation by large nearly neutrally buoyant particles. *J. Fluid Mech.* **712**, 41-60, doi: 10.1017/jfm.2012.393 (2012).

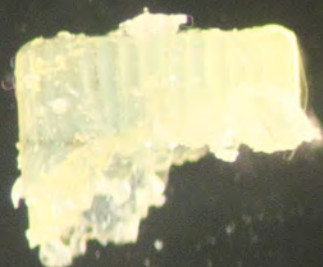
a)



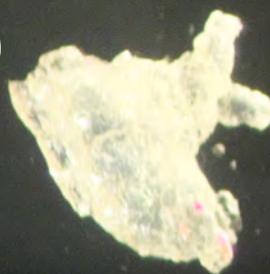
b)



c)



d)



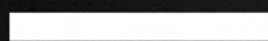
f)



e)



5 mm



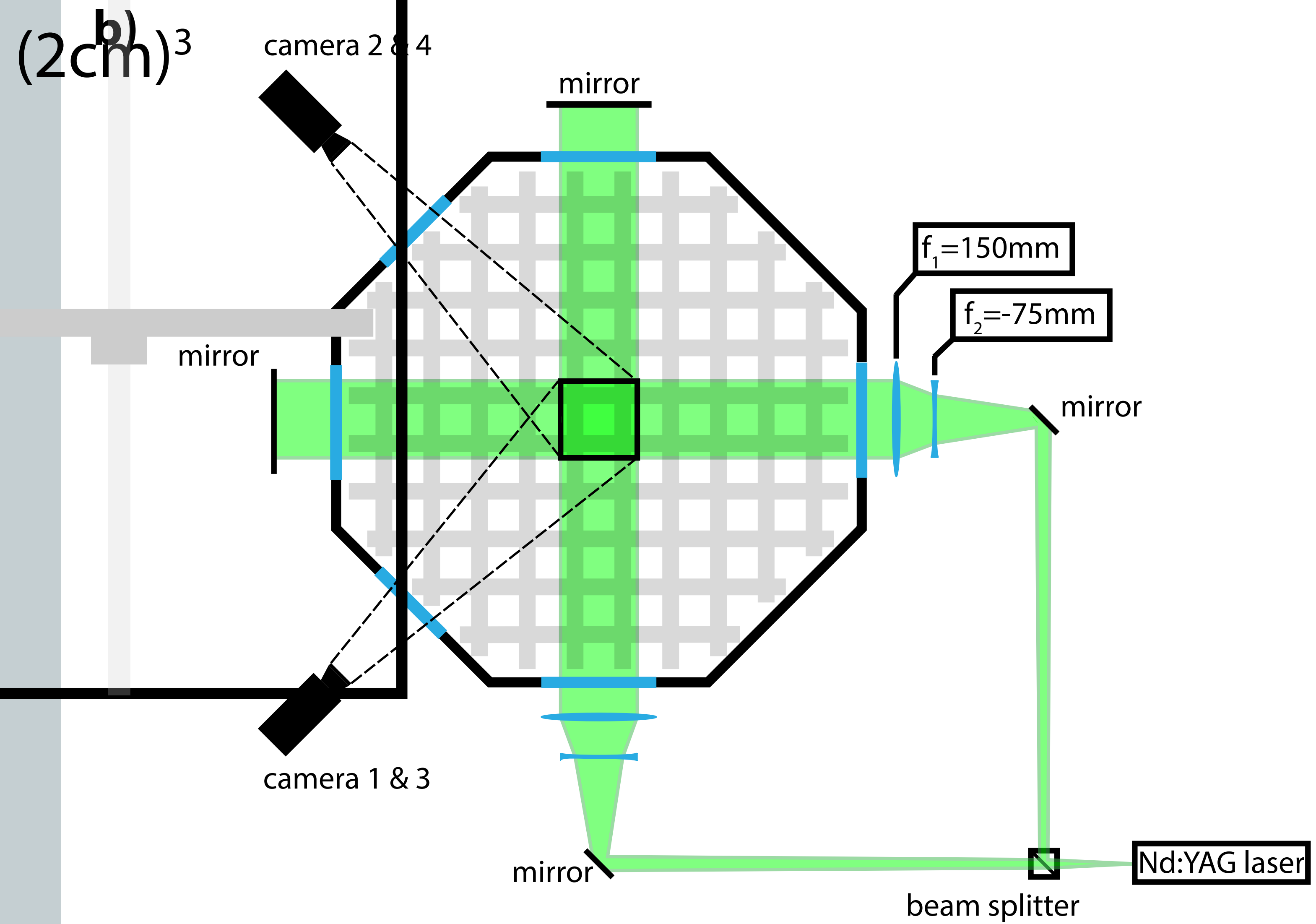
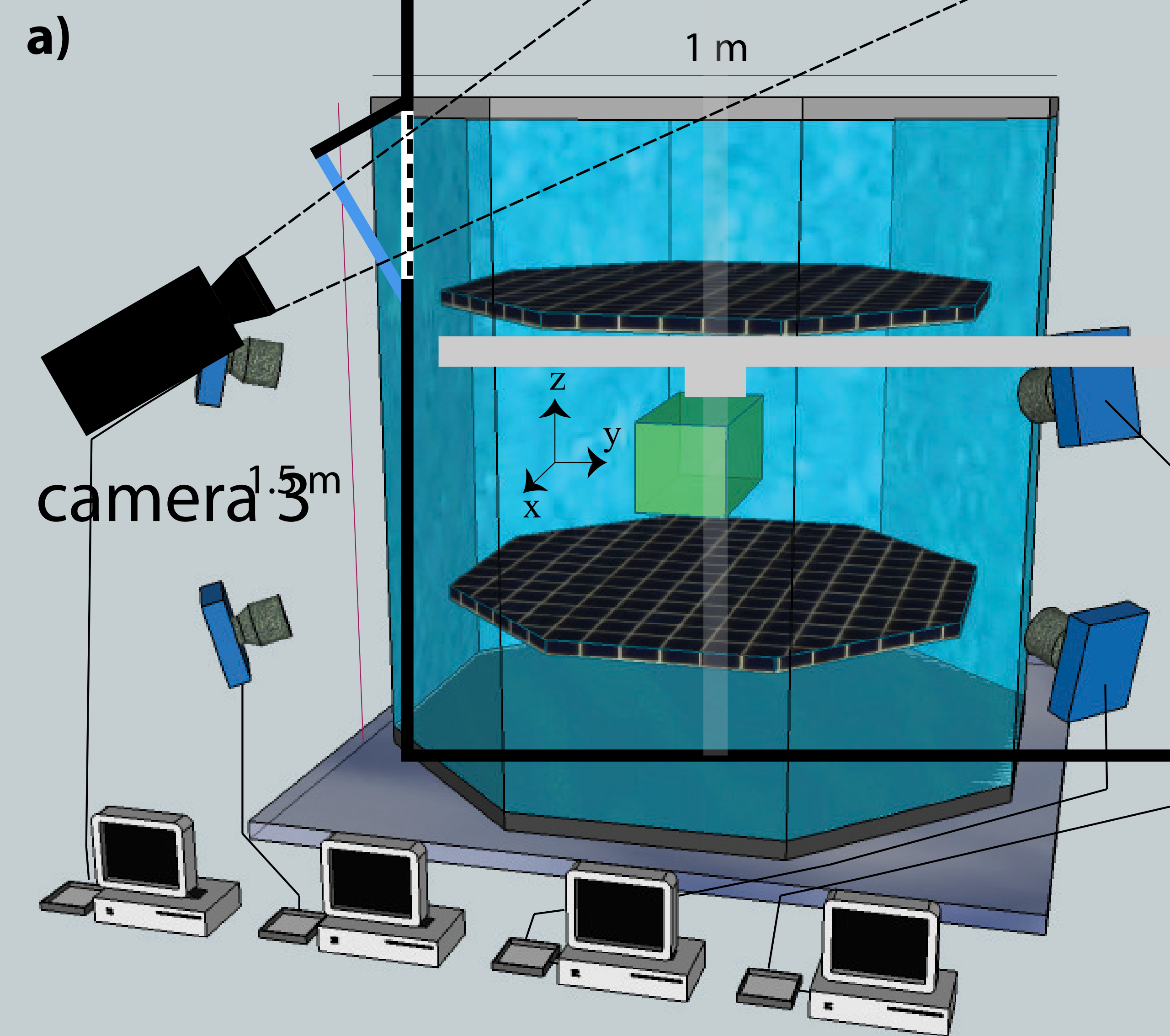


Figure 3

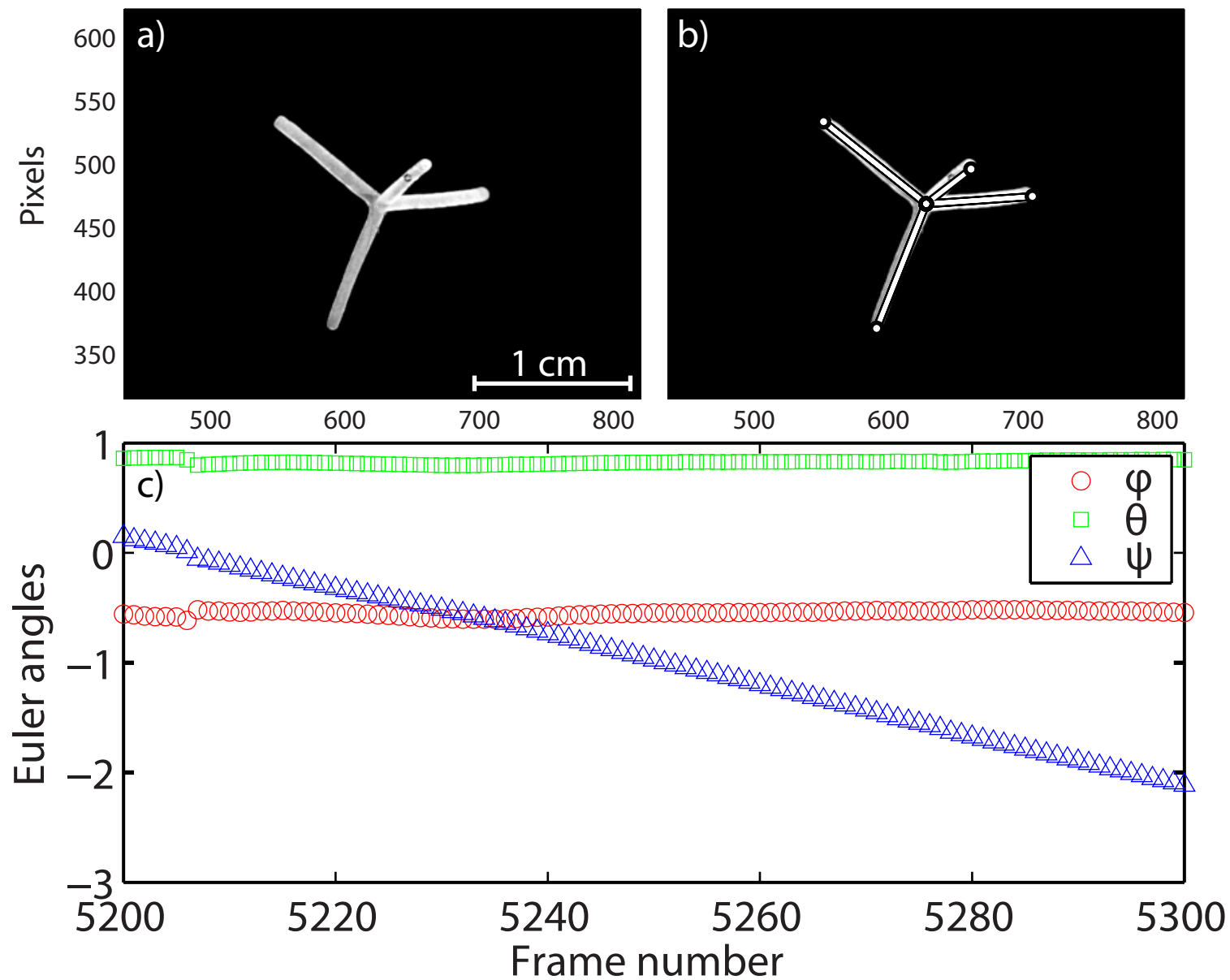
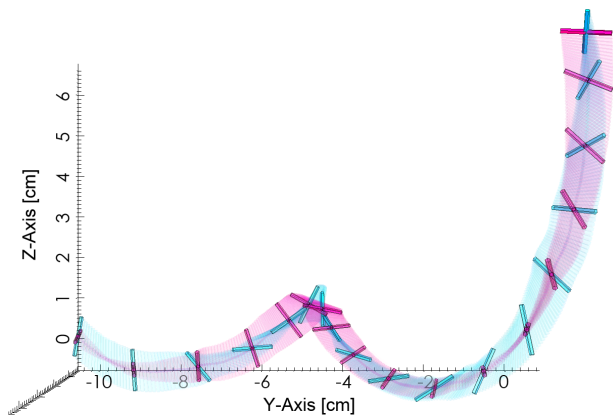
[Click here to download Figure Figure 3.pdf](#)

Figure 4

[Click here to download Figure Figure 4.pdf](#)



a)



b)

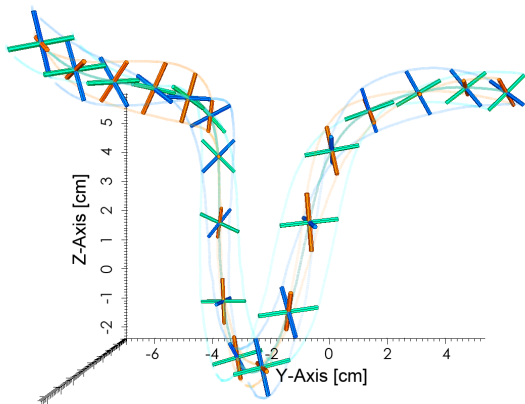
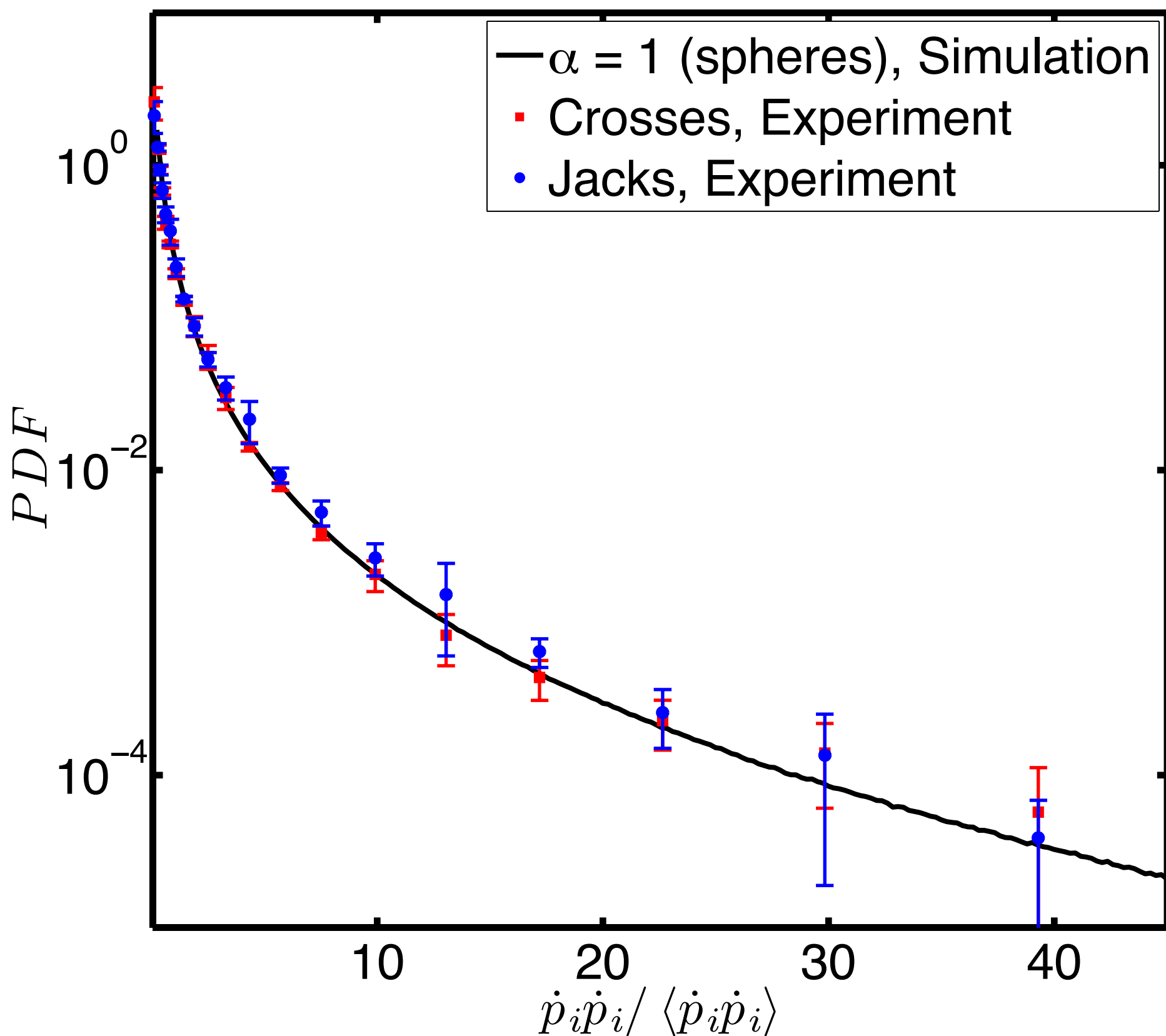
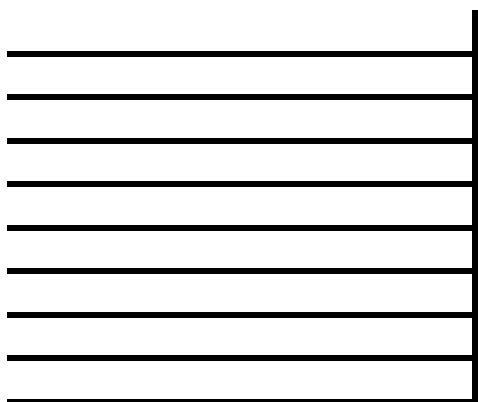


Figure 5



Name	Company	Catalog Number
Condor Nd:YAG 50W laser	Quantronics	532-30-M
High speed camera	Basler	A504k
High speed camera	Mikrotron	EoSens Mc1362
Rhodamine-B	ScienceLab.com	SLR1465
Sodium Hydroxide	Macron	7708
500 Connex 3D printer	Objet	
VeroClear	Stratasys	RGD810
Form 1+ 3D printer	Formlabs	
Clear Form 1 Photopolymer Resin	Formlabs	
Cylindrical and spherical lenses		
200, 100, 50 mm macro camera lenses		
Ultrasonic bath	Sonicator	
Calcium Chloride	Spectrum Chemical Mfg. Corp.	CAS 10043-52-2
LabVIEW System Design Software	National Instruments	
XCAP Software	EPIX	
MATLAB	Mathworks	
OpenPTV: Open Source Particle Tracking Velocimetry	OpenPTV Consortium	
ParaView	Kitware	
AutoCAD	AutoDesk	
Mesh with 0.040 x 0.053 inch holes	Industrial Netting	XN5170-43.5
Camera filters	Schneider Optics	B+W 040M

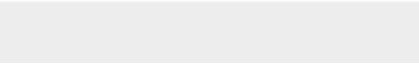

Comments
Pellets.
Used to make smaller particles. Particles ordered from RP+M (rapid prototyping plus manufacturing).
Objet build material.
Used to make larger particles.
F-mount.
Pellets.
Used to trigger cameras, control grid, and trigger laser.
Used with LabVIEW to trigger cameras.
Used for all image and data analysis. Programs for extracting 3D orientations from multiple images are included with this
Used to design all particles. Screenshots of particle designs are all of AutoCAD.





[Click here to access/download](#)

Animated Figure (video and/or .ai figure files)
makingatriad.mp4





[Click here to access/download](#)


Animated Figure (video and/or .ai figure files)
MATLAB_min.mov





[Click here to access/download](#)

Animated Figure (video and/or .ai figure files)
MATLAB_min_opt.mov





1 Alewife Center #200
Cambridge, MA 02140
tel. 617.945.8051
www.jove.com

ARTICLE AND VIDEO LICENSE AGREEMENT

Title of Article:

Methods for measuring the orientation and rotation rate of 3D printed particles in turbulent

Author(s):

Brendan Cole Guy Marcus Shima Parso Stefan Kraemel Rui Ni and Greg Voth

Item 1 (check one box): The Author elects to have the Materials be made available (as described at

<http://www.jove.com/publish>) via: ☒ Standard Access ☐ Open Access

Item 2 (check one box):

☐

The Author is NOT a United States government employee.

☐

The Author is a United States government employee and the Materials were prepared in the course of his or her duties as a United States government employee.

☐

The Author is a United States government employee but the Materials were NOT prepared in the course of his or her duties as a United States government employee.

ARTICLE AND VIDEO LICENSE AGREEMENT

1. **Defined Terms.** As used in this Article and Video License Agreement, the following terms shall have the following meanings: "Agreement" means this Article and Video License Agreement; "Article" means the article specified on the last page of this Agreement, including any associated materials such as texts, figures, tables, artwork, abstracts, or summaries contained therein; "Author" means the author who is a signatory to this Agreement; "Collective Work" means a work, such as a periodical issue, anthology or encyclopedia, in which the Materials in their entirety in unmodified form, along with a number of other contributions, constituting separate and independent works in themselves, are assembled into a collective whole; "CRC License" means the Creative Commons Attribution-Non Commercial-No Derivs 3.0 Unported Agreement, the terms and conditions of which can be found at: <http://creativecommons.org/licenses/by-nc-nd/3.0/legalcode>; "Derivative Work" means a work based upon the Materials or upon the Materials and other pre-existing works, such as a translation, musical arrangement, dramatization, fictionalization, motion picture version, sound recording, art reproduction, abridgment, condensation, or any other form in which the Materials may be recast, transformed, or adapted; "Institution" means the institution, listed on the last page of this Agreement, by which the Author was employed at the time of the creation of the Materials; "JoVE" means MyJoVE Corporation, a Massachusetts corporation and the publisher of *The Journal of Visualized Experiments*; "Materials" means the Article and / or the Video; "Parties" means the Author and JoVE; "Video" means any video(s) made by the Author, alone or in conjunction with any other parties, or by JoVE or its affiliates or agents, individually or in collaboration with the Author or any other parties, incorporating all or any portion of the Article, and in which the Author may or may not appear.

2. **Background.** The Author, who is the author of the Article, in order to ensure the dissemination and protection of the Article, desires to have the JoVE publish the Article and create and transmit videos based on the Article. In furtherance of such goals, the Parties desire to memorialize in this Agreement the respective rights of each Party in and to the Article and the Video.

3. **Grant of Rights in Article.** In consideration of JoVE agreeing to publish the Article, the Author hereby grants to JoVE, subject to Sections 4 and 7 below, the exclusive, royalty-free, perpetual (for the full term of copyright in the Article, including any extensions thereto) license (a) to publish, reproduce, distribute, display and store the Article in all forms, formats and media whether now known or hereafter developed (including without limitation in print, digital and electronic form) throughout the world, (b) to translate the Article into other languages, create adaptations, summaries or extracts of the Article or other Derivative Works (including, without limitation, the Video) or Collective Works based on all or any portion of the Article and exercise all of the rights set forth in (a) above in such translations, adaptations, summaries, extracts, Derivative Works or Collective Works and (c) to license others to do any or all of the above. The foregoing rights may be exercised in all media and formats, whether now known or hereafter devised, and include the right to make such modifications as are technically necessary to exercise the rights in other media and formats. If the "Open Access" box has been checked in Item 1 above, JoVE and the Author hereby grant to the public all such rights in the Article as provided in, but subject to all limitations and requirements set forth in, the CRC License.

ARTICLE AND VIDEO LICENSE AGREEMENT

4. Retention of Rights in Article. Notwithstanding the exclusive license granted to JoVE in **Section 3** above, the Author shall, with respect to the Article, retain the non-exclusive right to use all or part of the Article for the non-commercial purpose of giving lectures, presentations or teaching classes, and to post a copy of the Article on the Institution's website or the Author's personal website, in each case provided that a link to the Article on the JoVE website is provided and notice of JoVE's copyright in the Article is included. All non-copyright intellectual property rights in and to the Article, such as patent rights, shall remain with the Author.

5. Grant of Rights in Video – Standard Access. This **Section 5** applies if the "Standard Access" box has been checked in **Item 1** above or if no box has been checked in **Item 1** above. In consideration of JoVE agreeing to produce, display or otherwise assist with the Video, the Author hereby acknowledges and agrees that, Subject to **Section 7** below, JoVE is and shall be the sole and exclusive owner of all rights of any nature, including, without limitation, all copyrights, in and to the Video. To the extent that, by law, the Author is deemed, now or at any time in the future, to have any rights of any nature in or to the Video, the Author hereby disclaims all such rights and transfers all such rights to JoVE.

6. Grant of Rights in Video – Open Access. This **Section 6** applies only if the "Open Access" box has been checked in **Item 1** above. In consideration of JoVE agreeing to produce, display or otherwise assist with the Video, the Author hereby grants to JoVE, subject to **Section 7** below, the exclusive, royalty-free, perpetual (for the full term of copyright in the Article, including any extensions thereto) license (a) to publish, reproduce, distribute, display and store the Video in all forms, formats and media whether now known or hereafter developed (including without limitation in print, digital and electronic form) throughout the world, (b) to translate the Video into other languages, create adaptations, summaries or extracts of the Video or other Derivative Works or Collective Works based on all or any portion of the Video and exercise all of the rights set forth in (a) above in such translations, adaptations, summaries, extracts, Derivative Works or Collective Works and (c) to license others to do any or all of the above. The foregoing rights may be exercised in all media and formats, whether now known or hereafter devised, and include the right to make such modifications as are technically necessary to exercise the rights in other media and formats. For any Video to which this Section 6 is applicable, JoVE and the Author hereby grant to the public all such rights in the Video as provided in, but subject to all limitations and requirements set forth in, the CRC License.

7. Government Employees. If the Author is a United States government employee and the Article was prepared in the course of his or her duties as a United States government employee, as indicated in **Item 2** above, and any of the licenses or grants granted by the Author hereunder exceed the scope of the 17 U.S.C. 403, then the rights granted hereunder shall be limited to the maximum rights permitted under such

statute. In such case, all provisions contained herein that are not in conflict with such statute shall remain in full force and effect, and all provisions contained herein that do so conflict shall be deemed to be amended so as to provide to JoVE the maximum rights permissible within such statute.

8. Likeness, Privacy, Personality. The Author hereby grants JoVE the right to use the Author's name, voice, likeness, picture, photograph, image, biography and performance in any way, commercial or otherwise, in connection with the Materials and the sale, promotion and distribution thereof. The Author hereby waives any and all rights he or she may have, relating to his or her appearance in the Video or otherwise relating to the Materials, under all applicable privacy, likeness, personality or similar laws.

9. Author Warranties. The Author represents and warrants that the Article is original, that it has not been published, that the copyright interest is owned by the Author (or, if more than one author is listed at the beginning of this Agreement, by such authors collectively) and has not been assigned, licensed, or otherwise transferred to any other party. The Author represents and warrants that the author(s) listed at the top of this Agreement are the only authors of the Materials. If more than one author is listed at the top of this Agreement and if any such author has not entered into a separate Article and Video License Agreement with JoVE relating to the Materials, the Author represents and warrants that the Author has been authorized by each of the other such authors to execute this Agreement on his or her behalf and to bind him or her with respect to the terms of this Agreement as if each of them had been a party hereto as an Author. The Author warrants that the use, reproduction, distribution, public or private performance or display, and/or modification of all or any portion of the Materials does not and will not violate, infringe and/or misappropriate the patent, trademark, intellectual property or other rights of any third party. The Author represents and warrants that it has and will continue to comply with all government, institutional and other regulations, including, without limitation all institutional, laboratory, hospital, ethical, human and animal treatment, privacy, and all other rules, regulations, laws, procedures or guidelines, applicable to the Materials, and that all research involving human and animal subjects has been approved by the Author's relevant institutional review board.

10. JoVE Discretion. If the Author requests the assistance of JoVE in producing the Video in the Author's facility, the Author shall ensure that the presence of JoVE employees, agents or independent contractors is in accordance with the relevant regulations of the Author's institution. If more than one author is listed at the beginning of this Agreement, JoVE may, in its sole discretion, elect not take any action with respect to the Article until such time as it has received complete, executed Article and Video License Agreements from each such author. JoVE reserves the right, in its absolute and sole discretion and without giving any reason therefore, to accept or decline any work submitted to JoVE. JoVE and its employees, agents and independent contractors shall have

ARTICLE AND VIDEO LICENSE AGREEMENT

full, unfettered access to the facilities of the Author or of the Author's institution as necessary to make the Video, whether actually published or not. JoVE has sole discretion as to the method of making and publishing the Materials, including, without limitation, to all decisions regarding editing, lighting, filming, timing of publication, if any, length, quality, content and the like.

11. **Indemnification.** The Author agrees to indemnify JoVE and/or its successors and assigns from and against any and all claims, costs, and expenses, including attorney's fees, arising out of any breach of any warranty or other representations contained herein. The Author further agrees to indemnify and hold harmless JoVE from and against any and all claims, costs, and expenses, including attorney's fees, resulting from the breach by the Author of any representation or warranty contained herein or from allegations or instances of violation of intellectual property rights, damage to the Author's or the Author's institution's facilities, fraud, libel, defamation, research, equipment, experiments, property damage, personal injury, violations of institutional, laboratory, hospital, ethical, human and animal treatment, privacy or other rules, regulations, laws, procedures or guidelines, liabilities and other losses or damages related in any way to the submission of work to JoVE, making of videos by JoVE, or publication in JoVE or elsewhere by JoVE. The Author shall be responsible for, and shall hold JoVE harmless from, damages caused by lack of sterilization, lack of cleanliness or by contamination due to the making of a video by JoVE its employees, agents or independent contractors. All sterilization, cleanliness or decontamination procedures shall be solely the responsibility of the Author and shall be undertaken at the Author's

expense. All indemnifications provided herein shall include JoVE's attorney's fees and costs related to said losses or damages. Such indemnification and holding harmless shall include such losses or damages incurred by, or in connection with, acts or omissions of JoVE, its employees, agents or independent contractors.

12. **Fees.** To cover the cost incurred for publication, JoVE must receive payment before production and publication the Materials. Payment is due in 21 days of invoice. Should the Materials not be published due to an editorial or production decision, these funds will be returned to the Author. Withdrawal by the Author of any submitted Materials after final peer review approval will result in a US\$1,200 fee to cover pre-production expenses incurred by JoVE. If payment is not received by the completion of filming, production and publication of the Materials will be suspended until payment is received.

13. **Transfer, Governing Law.** This Agreement may be assigned by JoVE and shall inure to the benefits of any of JoVE's successors and assignees. This Agreement shall be governed and construed by the internal laws of the Commonwealth of Massachusetts without giving effect to any conflict of law provision thereunder. This Agreement may be executed in counterparts, each of which shall be deemed an original, but all of which together shall be deemed to be one and the same agreement. A signed copy of this Agreement delivered by facsimile, e-mail or other means of electronic transmission shall be deemed to have the same legal effect as delivery of an original signed copy of this Agreement.

A signed copy of this document must be sent with all new submissions. Only one Agreement required per submission.

CORRESPONDING AUTHOR:

Name:

Greg Voth

Department:

Physics

Institution:

Wesleyan University

Article Title:

Methods for measuring the oriented advection rate of 3D printed particles in

Signature:

Greg Voth

Date:

4-17-2015

turbulence

Please submit a signed and dated copy of this license by one of the following three methods:

- 1) Upload a scanned copy of the document as a pdf on the JoVE submission site;
- 2) Fax the document to +1.866.381.2236;
- 3) Mail the document to JoVE / Attn: JoVE Editorial / 1 Alewife Center #200 / Cambridge, MA 02139

For questions, please email submissions@jove.com or call +1.617.945.9051

Response to the Editor about “Methods for Measuring the Orientation and Rotation Rate of 3D-Printed Particles in Turbulence”

1. For steps 5.1.3 and 5.1.5, we will need the user input commands used (File | Save | etc.) in order to film this properly. The current instructions in the protocol state what to do but not how to do it. You state that nothing is being clicked in the analysis, but how is the analysis started? If you wish to use screen recordings in the video, we will need these files now in order to properly script and plan your video. Please include it with an updated Scriptwriter’s guide. Furthermore, please include the supplementary files now as well. All coding files/scripts to be provided upon publication should be sent at this point.

This has been addressed by adding a step under 5.1.3: “Click ‘Run’ to begin analysis.” The supplemental programs will make it clear that 5.1.5 is initiated as well by this step, so there is only one place where clicking Run is needed. The supplemental programs and video files have all been included with the submission, as has an updated Scriptwriter’s guide with improved screen recordings. These screen recordings are also included separately with the submission because it seems that they may not be attached to the Word document as they are supposed to be. They are included in the submission with the same file name as they are designated with in the Scriptwriter’s guide.

2. For Figure 5, please state whether the uncertainty is standard deviation, standard error of the mean, etc.

We have given more detail about what was done to arrive at the uncertainties. The error bars measure errors due to the bin sizes of the histogram and the fit length dependence of the particles’ rotation rate measurements. The fit-length dependence is shown in Marcus, 2014.

3. Please explicitly discuss future applications of the protocol in the Discussion. The critical steps have been addressed by the decision to use the tetrads.

This has been done. A paragraph has been added discussing extensions of these methods to much larger particles, which is research that we are actively conducting, as well as extensions to a variety of particle shapes.

JoVE Manuscript Changes: Responses to Comments by the Science Editor.

Manuscript title: “Methods for Measuring the Orientation and Rotation Rate of 3D-Printed Particles in Turbulence”.

Formatting note:

- Editor comment.
 - Response.

Edits made in response to comments from the editor:

- Please take this opportunity to thoroughly proofread the manuscript to ensure that there are no spelling or grammar issues. The JoVE editor will not copy-edit your manuscript and any errors in the submitted revision may be present in the published version.
 - Done.
- Continuity: Please highlight additional steps in section 1 (1.1.3-1.1.5) to include how some of the shapes were made in more detail for the video.
 - Done. Steps 1.1.3 – 1.1.5 have been highlighted.
- Formatting: All figures should have a title and a short description in the legend.
 - Bolded portions of the figure descriptions that would serve as their titles and added a title to Figure 5.
- 2.3.3. – How are ~250 particles measured out?
 - After reviewing the manuscript, we realized that this number should have been ~2,500, not ~250. This has been corrected, and “enough to loosely fill ~25 mL in the density-matched storage solution” has been added to the manuscript.
- 3.1.3 – Approximately what angles? “Large” is not precise.
 - Clarified by adding “(~90°)” to the step.
- Please include a figure with an image of the setup showing the position of the laser and mirrors. This could be included as a supplementary figure.
 - We have added a part b to Figure 2 showing a top view of the apparatus with the illumination beam and the mirrors.
- 4.4 – How many particles are added?

- Clarified by changing “add all of those particles” to “add all 10,000 of those particles”.
- 4.4.2 – Does this synchronize the cameras? If so, how?
 - Clarified by adding “Use the external trigger to ensure all cameras start acquisition simultaneously and remain synchronized throughout the recording.”
- 5.1.3.1/5.1.5.1 – If this is to be filmed, please provide some direction as to what is being clicked in the software for this analysis.
 - Screen recordings of the analysis will be in the video. There is nothing being clicked in the analysis; it is a set of automatic programs that identify “tracks” where a particle is in view and fit a model orientation to the cluster of bright pixels seen on each camera, as is outlined in the manuscript. These programs will be included with the final manuscript along with sample image files.
- Please define the error in Figure 5 in the legend.
 - Done. Added “Measurement uncertainty accounts for random error from limited number of samples as well as the systematic error that results from the fit length dependence of the tumbling rate measurements.” to the legend.
- Discussion: Please discuss the critical steps and future applications of the protocol.
 - Have added a paragraph justifying the fitting used in 5.1.6 of the Protocol and have expanded two of the other paragraphs to include a more comprehensive review of critical steps and alternative methods.

JoVE Manuscript Changes: Responses to Comments by Reviewer 1.

Manuscript title: “Methods for Measuring the Orientation and Rotation Rate of 3D-Printed Particles in Turbulence”.

Formatting note:

- Reviewer comment.
 - Response.

Edits made in response to comments from the reviewer:

- Although the authors present another key concept of 3D printing as a central one, it seems to be not necessary to specify which method the users might find useful to create their particles: molding, printing, micro-machining or lithography, to name a few.
 - We agree that many different fabrication methods are possible. JoVE wants authors to focus on the specific methods used in a specific experiment and that is why the paper is written as it is.
- Another confusion that comes from the abstract is “Methods for producing on the order of 10,000 fluorescently dyed particles are described.” It is not clear why we need the methods also for fluorescent dyed particles and even more unclear is the 10,000. What if we just measure the motion of 1 or 100 particles or we need 100,000 particles?
 - Added a few lines to the Discussion to address why relatively low particle concentrations were used in these experiments. This paragraph, which is about the utility of the image compression systems, also addresses why it is beneficial in this apparatus to have on the order of 10,000 particles instead of just 1 or 100. We agree with the referee that a more general style is standard in our field, but JOVE wants precision about the experiments done.
- It continues with “four simultaneous video images” - what does it mean? four video cameras are involved? are these synchronized?
 - Clarified the phrasing in the abstract by changing “four simultaneous video images” to “four synchronized videos”.
- how tight is the synchronization requirement?

- External trigger on cameras provides synchronization at the level of a few microseconds and is much more than enough for our purposes here.
- Although the title claims that the flow is “turbulent”, the abstract says “low-Reynolds” - does it mean that we need to adjust the title to the low-Reynolds turbulent flows?
 - The Reynolds number is too low to have an inertial range in the Eulerian structure functions, but is still high enough that the flow is fully turbulent.
- I would strongly suggest to improve the abstract’s clarity.
 - The abstract’s phrasing and terminology have been improved.
- Another general statement is the specificity of the experiment presented - the flow is quite synthetic (grids, specific size, oscillating in phase, homogeneity, etc.) and not clear why the users cannot use different camera arrangements, different image software, different tracking software? After all, the paper is well prepared, the method is explained thoroughly and could be definitely made less explicit and applicable for more general cases. If it’s understood correctly, the general statement suggests that if we’d use a rod-type balloons connected together in a jack form, we could measure rotation of a hot gas in a ventilation system.
 - See response to the comment about step 1.1.1 of the Protocol, below.
- 9. Is there any additional information that would be useful to include? yes, the software code of calibration, tracking, rotation assignment, Euler angles and solid body rotation rates. if compression is necessary, then it is also required for the users to be able to replicate the experiment.
 - Many of these will indeed be included with the final manuscript.
- 11. Are any important references missing and are the included references useful? yes, some references are missing and some are corrupted. the suggestions are given below
 - References have been fixed.
- abstract: “any shape that can be modeled on a computer using multiple slender rods” I’m not sure that it really means “any shape”. It is more likely that some shapes, although can be modeled by slender rods will not doable, if, for instance, the rods will start obscure each other from the cameras (a sort of a optical density measure).

- This is true, and shadowing due to arms is addressed in the Discussion. We largely rewrote this paragraph.
- p2 170 “and the rotational motions of these particles are identical to those of their respective effective ellipsoids” - without going deeper into literature I would claim that this is only partially true - the effective force and moment on a particle is a surface integral over a solid surface of a particle and not an integral over an “equivalent” volume of a fluid which might also have some flux out of the volume of an “effective ellipsoid”. Whether the behavior is identical or not, remains to be studied in more details in each separate case, definitely in turbulent flows. It is suggested to add a clear statement about the degree of applicability that is not known *a priori* and shall be studied carefully by the users of this method. It relates to the following statement “Particles with symmetric arms of equal length rotate like spheres.” - in some sense the authors mean that the symmetric arms experience a symmetric forces and moments, similarly to the sphere, but definitely not the same ones. It could be that the authors mean that the size of the particle is also a parameter and maybe for very small particles (the size of which I could not deduce right now) this statement is more correct, than for large particles. Although the simulation of spheres compared to the rotation rates of jacks and crosses show indeed the similarity, it does not mean at all that instantaneously these bodies would rotate similarly. Statistically, they do experience a similar rotation rate, but that is a *completely different statement*.
- This is covered in reference [2], where it is shown that small axisymmetric particles composed of slender arms have dynamics in turbulence equivalent to those of corresponding ellipsoids, called “corresponding effective ellipsoids” in the manuscript. It is indeed rigorous, but only true for small particles for which the velocity gradient is uniform across the particle. For larger particles that the referee seems to be referring to, the rotations indeed depend on shape in much more complicated ways.
- p2 184 “ Extension of these methods to tracking rods was done by Parsa et al [5]” - I have looked for some information in ref. [5] (the journal is not given, but a quick Google search reveals it's also in PRL, 2012) and ref. [6], but could not find any relevant information regarding of this statement “extension was done”. The references do not explain what extension was done or how it is done, except that the rotation rates are fitted with quadratic

formula. There are two things to correct here: a) provide actual information on how the tracking methods of refs [3,4] are extended in order to provide the rotation rate measurements. b) why quadratic formula is used and how this affects the results.

- Apologies about the incomplete reference. Issues related to references have been fixed.
- This paragraph has been edited to clarify the relation of Parsa, *et al* to previous experiments and to the measurement methods presented here. Parsa, *et al* used stereoscopic images from multiple cameras to track the position and orientation of rods in turbulence, and the quadratic formula mentioned in that publication is simply the way the data was smoothed. It is unrelated to the measurements and methods discussed in this manuscript.
- Protocol: 1.1.1. why the slender diameter is 0.3 mm and why the length is 3 mm?
 - Earlier versions of this manuscript provided more leeway within the experimental procedure, but the editors wanted it to be more definitive and confined to our specific experiments. The procedure here details how these specific experiments were done, but we acknowledge that similar results could have been found with many types of turbulent flows, particles, and experimental apparatus.
- 1.1.6 - why is it 3D printer involved? and not some other production method? I'd say it's redundant in a view of suggestion 1.2 - order ...
 - See previous response.
- 1.2.1 this is very important to understand what is the reason for "Ensure that particles are printed on high-resolution mode." It is important for the users to know what does the "high resolution" means from the practical point of view of the experiment? the surface roughness? the length of the rods? the diameter? the connectivity in the center? the symmetry?
 - Clarified with the addition of the following: "[print on high-resolution mode] because the particles are near the minimum feature size of many 3D printers and the arms will not be as symmetric and may break if printed at lower resolution."
- 2.1 - probably instead of "Prepare water in which the particles are neutrally buoyant." - prepare a liquid in which the particles are neutrally buoyant.

- Changed “water” to “a salt solution”.
- or maybe even prepare an experiment - why the issue of measuring rotation rates has to deal with the question of buoyancy? if the users would like to implement the method in air and prepare the particles inflatable with helium? or use them in a positively or negatively buoyant conditions?
 - We have studied the neutrally buoyant case. There is a lot of interesting physics in non-neutrally buoyant particles, and there are many ways to adjust particle buoyancy. At this point in the process, we just need neutrally buoyant particles for processing.
 - We added “to minimize particles’ arms bending while in storage and so that gravitational and buoyancy forces do not have to be accounted for in the analysis”.
 - See also response to the comment about step 1.1.1.
- 2.1.1.2 “different water densities” - probably “different solution densities”
 - Changed “water” to “solution”.
- 2.1.3 - not clear at all how the authors know how much salt (and of what type, maybe one would use magnesium salts?) to mix with what solvent (why water?) to get the density of the particles?
 - This is found through a calculation involving the density of the water and of the CaCl_2 that we did not include in the manuscript.
- Why not to print the hollow particles that might even float in water?
 - We are interested in the neutrally buoyant case for the reasons included in the addition to step 2.1: “so that gravitational and buoyancy forces do not have to be accounted for in the analysis”.
 - Hollow particles could have densities that change with time as water diffuses in, making analysis and interpretation of results more difficult. See the second response to the comment about the note after step 2.2.4.
- in 2.1.4 the temperature is mentioned for the first time - I’d suspect the temperature has a lot of significance in all the discussed experiment’.
 - Storage temperature, within reasonable limits, does not have much of an effect in these experiments. This detail, “at room temperature”, was

included because in an earlier draft of the manuscript we were asked to include the temperature at which the particles are stored.

- 2.2. this item is completely not clear. what is the resin and what are the small sections and...
 - Changed the beginning of this step to say, “Manually loosen the support material in which the particles come encased by gently...”.
- what is “manually massage”
 - This will be shown in the video.
- wouldn’t the NaOH solution remove all the resin without this preparation step? is it only for a specific printing material?
 - Clarified why manually removing some of the resin is done: “Remove excess resin in this way to reduce the amount of the NaOH solution that will need to be created for steps 2.2.1 – 2.2.4.”
- this is a very interesting note: “If particles are not stored in a density-matched solution, some arms may bend. Keeping them immersed in the density-matched solution for several hours also allows some voids in the plastic to fill with fluid.” first the bending - how the user would verify that the arms are not bend somewhere along the handling process? and how does one assure that the rotation rates later on are not measured for a biased subset of particles?
 - We have looked carefully at random samplings of a large number of our particles under a microscope in order to check that storing them in a density-matched solution minimizes bending. Some arms, of course, do have small deviations due to the handling process and these particles end up giving worse orientation matches.
- Second, if there are cases where particles are used with voids - their buoyancy is different and their interaction with the fluid is different also (e.g. an air cushion around it? small bubbles released when particles move?) - have the authors noticed something of this kind?
 - We have noticed that particle densities change with time over the course of being stored in density-matched solutions and have interpreted this as the salt solution filling voids in the particles. Part of the reason that we store the

particles before performing the experiments is to have as many of these voids filled as possible before experiments begin.

- what does it mean “Dye particles with Rhodamine-B mixed with water” ? if the liquid is not water anymore, but some saline solution - is it possible to dye the particles? is Rhodamine B adhesive to the particles that spent some time in the bath with NaOH? is the 0.5 g/L a normal concentration of the Rhodamine B for any kind of particles?
 - The 0.5 g/L concentration of Rhodamine-B was arrived at by testing different concentrations, as were the duration and temperature of the dyeing.
 - For more recent experiments with softer plastics, we have tried dyeing particles in Rhodamine-B mixed with a salt solution in which the particles were neutrally buoyant. The dye enters the particles just as well in a salt solution as in a water solution.
- The heating of the whole thing is also questionable in a view of the previous discussion of the bending of particles and density matching.
 - Clarified this by adding “using too high of a temperature will result in the arms bending.”
- 3.1.1 what are these requirements for? 1 megapixel and 450 fps? is it for any Reynolds number turbulent flow? Can the user use some other cameras for different purposes?
 - See response to the comment about step 1.1.1.
- it is not clear (as the rotation tracking is not described clearly) why “Using more than four cameras could likewise decrease orientation measurement uncertainty.” shouldn’t redundancy help in this case?
 - Added to the end of this step to clarify this point: “Using more than four cameras could likewise increase orientation measurement precision because it will reduce the chance of arms being shadowed on all cameras, which is a primary source of uncertainty.”
- 3.1.3 why “Minimize optical distortions by building viewing ports into the apparatus perpendicular to each camera viewing direction” this requirement is important? how the distortions affect the rotation measures?

- In tracking small spherical tracers we have found small (~20 micron) stereomatching errors when we look obliquely through a window into the apparatus. For the rotation measurements we have only used perpendicular viewing, but we expect that oblique viewing would very slightly degrade orientation measurements.
- 3.1.4 - why 200 mm macro lenses? these are extremely expensive lenses? why other lenses wouldn't work?
 - Added "to obtain the desired measurement volume from a working distance of half a meter" to clarify the reasoning behind choosing these lenses.
 - These are expensive lenses, however they are still much less expensive than the cameras.
 - See also the response to the comment about step 1.1.1.
- is the size of the volume limited only to 3 x 3 x 3 cm?
 - This is a reasonable compromise between the desire to have high-resolution images of the particles and to track them over long periods of time.
- 3.1.5 - how does the mask look like? is it specific for rotation measure?
 - The mask is simply a grid of points used to identify common points on each camera and thereby create a common 3D coordinate system for all four cameras. It is not specific for rotation measure.
 - The mask will be shown in the video.
- 3.1.5.3 what is this aperture ? #f11 ? why are the filters? what are these B+W 040M 4x filters? why the filters are positioned after the calibration?
 - Corrected the order of the procedure; filters should be positioned before the calibration is done. Thank you for pointing this out.
- why do we need those?
 - We need to filter out the green 532 nm light from the laser, which would otherwise obscure views of the particles.
- the references are incorrect on p. 6 l271 OpenPTV is ref. [4] and Ouellette is ref [3].
 - References have been fixed. Apologies for the difficulty.
- 3.2 - the use of the laser and fluorescent particles is not clear at all. the power of the laser has probably little effect as the light collected on the cameras is the fluorescence of

Rhodamine? it's also related to the later statement of triggering of the laser and the cameras at 450 Hz. Does it mean that the laser should be extremely powerful (Q-switched Nd:YAG with 50 W and

- The laser power is spread out into a large area (the size of the viewing volume), so the fluorescence is not saturated by the incoming light. We have varied the laser intensity within our accessible range and find that the fluorescence intensity does not saturate in this range.
- also not clear why the users in this method are instructed to follow the homogeneous portion of some flow (and why ref. [8] is relevant?) what if the user measures rotation in a jet?
 - We have been interested in homogeneous flows. [8] discusses the homogeneity of this flow and the limits to the assumption of complete homogeneity. We also think these methods would be useful in inhomogeneous flows.
 - See also response to the comment about step 1.1.1.
- how item 4.1.1 relates to this method? what if the users do not have image compression system at all?
 - After reading the Discussion, the reviewer commented, “the image compression need is clear now (ignore the comments above)”.
- what if the users would use another type of tracking system? a commercial one? or another real time image compression types, for instance by Kreizer et al (Exp. Fluids 2010, 2011)? it is interesting to understand whether the same principles will work with the defocusing, or astigmatism tracking systems (Kahler, Cirpka, etc. Exp. Fluids 2012, 2014)
 - See the response to the comment about step 1.1.1. The methods detailed in this paper are not the unique ways to experimentally arrive at these results; they are the methods we used in these experiments.
- the note “Because each particle typically covers approximately 5,000 bright pixels” really confusing - 5000 pixels each particle? does it mean that in the volume one shall have 5 to 10 particles in a time?
 - This is partially explained later in that same sentence and in the Discussion: “there is rarely more than one particle in view at a time” (from the note) and “Particle concentrations in these experiments were about $5 \times 10^{-3} \text{ cm}^{-3}$,

which meant that typically only about 20% of images from the cameras had a particle” (from the Discussion).

- We use a small field of view in order to obtain a large number of pixels for each particle in order to obtain highly accurate orientation measurements.
- 4.2 - again, why the setup is so specific? why 1 x 1 x 1 m? why turbulent by two parallel 8 cm mesh grids? why in phase?
 - See response to the comment about step 1.1.1.
- recording items again have a lot of very specific details which will likely be irrelevant for most of the users.
 - See response to the comment about step 1.1.1.
- 5.1.3 - 5.1.3.1 are probably some key components that will help to deduce the orientation of the particle. this would be very useful to understand what are the “numerical models” - is it the light spreading/diffraction of the rods which are modeled?
 - Clarified this step by changing the sentence to “Using the camera calibration parameters from 3.1.5.6, project the two end points of each rod onto the cameras and then model the distribution of light intensity in two dimensions...”.
 - Also broke this up into two steps to help clarify.
- not clear from the description of 5.1.4-5.1.5 what is the orientation of the particle and whether the problem is ill-defined as the same particle can have symmetrical orientations that are all fitted?
 - This is the concern motivating step 5.1.6. We have also added a paragraph to the Discussion justifying this assumption.
- does it have any meaning for the following result if the rod positions are switched? i.e. if the particle is slightly not symmetrical and it's a cross but of uneven length (an elliptical disk model) - how difficult it would be to orient the two axis of the ellipse?
 - This would be an interesting avenue to pursue but we so far have only used symmetric particles. This method could be used to track asymmetric particles, in which case this step would need careful attention.
- especially difficult seems to be the choice of 5.1.6 - are there any false results? any uncertainty with one the steps above?

- Addressed this by adding a paragraph to the Discussion justifying the smoothing assumption in 5.1.6. Mean rotation rates are more than an order of magnitude below the threshold that would make false results an issue.
- p5 1453 again “Small jacks rotate just like spheres in fluid flows” shall have somewhere “statistically” or “on average” or “rotation rates distribute similarly to”
 - See the response to the comment about this in the Introduction. A small jack in a uniform velocity gradient rotates exactly like a sphere.
- p11 1490 “Traditionally, the fluid vorticity has been measured using complex, multi-sensor, hot-wire probe” - this is probably true only for “single point”. Otherwise, “traditionally” the same 3d tracking methods were used by the ETH Zurich group to show vorticity (and moments of vorticity) and longer before that by Dahm using scalar imaging, etc. Probably there are other methods that measured vorticity, like LDV, etc.
 - References to these groups have been added in the paragraph, but as the reviewer mentions it is very difficult to have a comprehensive review of the field, which is why ours is primarily focused on other methods of particle tracking.
- p11 1500 “3D-printed anisotropic particles can be small, down to 300 μm in diameter” - this statement is somewhat different from the size given in the CAD program?
 - We think it is consistent throughout that particles have 3 mm arm length and 300 μm arm diameter. Also clarified the Discussion: “3D-printed anisotropic particles can be small, with arm thicknesses down to .3 mm in diameter”.
- p12 1525 ... However, the shape of tetrads is not shown
 - They will be shown in the video. A screenshot of the tetrad was also included with the previous submission.
- and it's also not clear whether the particles can be cubes or pyramids, i.e. not connected at the center?
 - These particles have been considered, but we decided not to pursue them because parts of these objects shadow one another more often. We expect that these methods could be used with a wide variety of particle shapes.
- Regarding the surface of the particle as one of the key parameters in adequate correspondence of the rotation to the real case of a spheroid, the question is how the results

are similar/different if the jack/cross is embedded in a transparent ball? this can be a good verification of the general statement of “equivalence of rotation rates” and the processing method.

- We agree that this is an interesting approach. The Bodenschatz group (MPI Gottingen) and the Variano group (Berkeley) have done experiments like this. We are quite confident in the Stokes flow solutions that show that equivalent spheroids have identical rotations in uniform velocity gradients. (See Bretherton JFM 14:284 1962 and Marcus et al, NJP (Ref 1) for details).

JoVE Manuscript Changes: Responses to Comments by Reviewer 3.

Manuscript title: “Methods for Measuring the Orientation and Rotation Rate of 3D-Printed Particles in Turbulence”.

Formatting note:

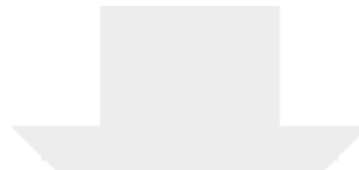
- Reviewer comment.
 - Response.

Edits made in response to comments from the reviewer:

- Step 2.2 This step seems sensitive to the specific manufacturer. You did list this in Table 1, but it could help also to list the 3D manufacturing technique generically, e.g. “We used a proprietary polymer with bulk density of X that is built by laser-sintering of dry powder, with minimum resolution of 200 microns.”
 - Yes, step 2.2 is very dependent on the type of printer used. We added a sentence to 1.2 to help clarify. The editors have a set of requirements that prevent us from specifying the commercial printer we used in the text (only in the table) and also want us to be very specific about exactly how the experiments were performed. In this case, it is essentially impossible to meet both of these requirements.
- Line 180 Consider replacing the word “base” with “NaOH solution”
 - Done.
- Line 205 “extensive” may not be the best word choice here
 - Fixed. Changed “prevent extensive loss of dye” to “prevent losing a detrimental amount of dye”. It is hard to quantify what an acceptable amount of dye lost would be, as the ultimate test of the dye is the degree to which it fluoresces under the laser. This should be tested before experiments have begun.
- Line 259 Mention the word “aperture” in connection with the value f11 (or f/11).
 - This now reads “Set the apertures to f/11 and mount...”
- Line 259 Describe these filters generically, e.g. “532nm notch filters” or “neutral-density filter.” Also, B&W is a brand name, and you generally save those for table 1.
 - This has been changed to “532 nm notch filters to remove laser light while allowing through longer-wavelength fluorescence onto the cameras”.

- Line 260 check the grammar
 - Thank you for noticing the mistake. Changed “Be careful to change as little about the optical setup from this point forward” to “Be careful to change as little as possible about the optical setup from this point forward.”
- Step 3.1.5.7 I think this step requires more guidance. Either add a few sentences or add a citation to other work describing it in more detail.
 - Yes, there is a lot included in that step. We extended the description and included references to two sources that describe how this is done.
- Line 279 Specify the repetition rate at which the laser exhibits this average power. If the laser has a different average power at 450 Hz, please indicate that as well.
 - We added a note to the end of 3.2: “Note: The laser power is specified at a pulse frequency of 5 kHz. The pulse frequency in these experiments is 900 Hz, where the output power is significantly lower.”
 - The ambiguous language of step 4.4.2 has also been changed, from “Set cameras and laser to respond to an external trigger and set the frequency of the trigger to 450 Hz” to “Set cameras and laser to respond to an external trigger and set the frequency of the trigger to 450 Hz for the cameras and 900 Hz for the laser.”
- Steps 4.4.5 and 4.4.6 Consider saying explicitly that you check the set of 10^6 images for quality before proceeding to step 4.4.7
 - Done.
- Line 365 because the geometric regularity is invoked here, I think that the claim of "arbitrary shape" as indicated on line 86 is either overstated, or needs more discussion.
 - More careful language has been used in line 86: “arbitrary shape” has been changed to “a wide variety of shapes”.
 - For particles that were not as symmetric as those in these experiments, methods similar to these could still be used for finding their positions and orientations. More care would just have to be taken when finding the center of the particle, since, as is implied in this comment, the optical center of bright pixels would not necessarily be the center of the particle.
- Line 409-410 I think it would be cool to see a model image corresponding to the fit in image 3b.

- This is something that will be included in the video.
- Euler angles - because the term "Euler angles" is often used loosely or incorrectly, it is helpful to be very explicit about what orientation convention you use. For example, you can say "phi, theta, and psi represent subsequent rotations about X,Y, then Z axes, which are fixed in the lab frame" or "phi, theta, and psi represent subsequent rotations about the particle's X,Y, and then new X axis"
 - A note has been included after 5.1.5.1 that clarifies the Euler angle convention used in these experiments and analyses.
- Line 440 I would like to see the “more recent work” cited, or expanded upon here.
 - This work not yet been published. We have slightly extended this description, but full specification of how to do the least squares fit seems beyond the discussion here.
- Line 504 I don’t understand what you mean by “A higher volume of measurements”
 - The phrasing was confusing. Changed “A higher volume of measurements” to “Having more measurements”.



[Click here to access/download](#)

Supplemental File (as requested by JoVE)
Updated Scriptwriters Guide.docx





[Click here to access/download](#)

Supplemental File (as requested by JoVE)
NJP copyright statement - New Journal of Physics -
IOPscience.pdf

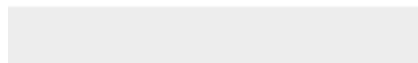
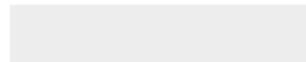




[Click here to access/download](#)

Supplemental code file (if applicable)

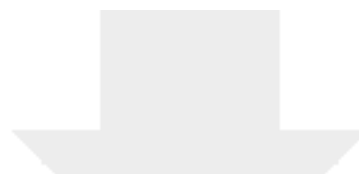
Use_Instructions.txt





[Click here to access/download](#)

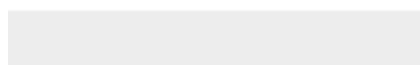
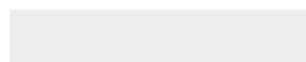
Supplemental code file (if applicable)
Organize_Files.m

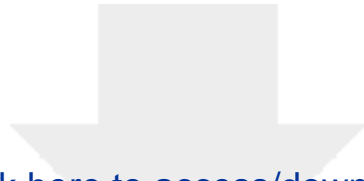


[Click here to access/download](#)

Supplemental code file (if applicable)

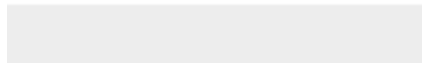
README_rot.txt





[Click here to access/download](#)


Supplemental code file (if applicable)
dynamic_camParaCalib.mat

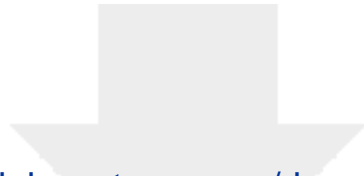




[Click here to access/download](#)

Supplemental code file (if applicable)
`sk_read_cpv.m`



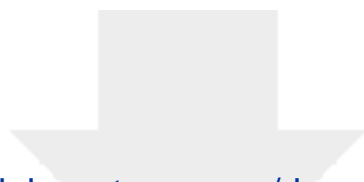


[Click here to access/download](#)

Supplemental code file (if applicable)

`sk_remove_bad_frames.m`

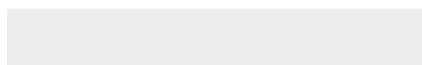
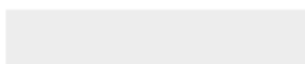




[Click here to access/download](#)

Supplemental code file (if applicable)

README_ori.txt





[Click here to access/download](#)

Supplemental code file (if applicable)
`write2_gdf.m`

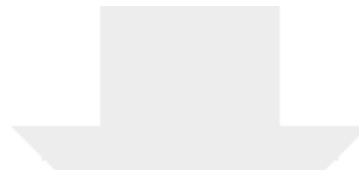


[Click here to access/download](#)

Supplemental code file (if applicable)

bc_sk_find_particles.m





[Click here to access/download](#)

Supplemental code file (if applicable)

`find_clusters.m`

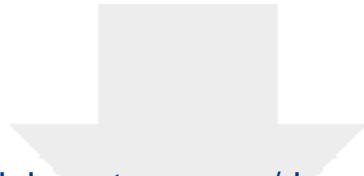




[Click here to access/download](#)

Supplemental code file (if applicable)
read2_gdf.m

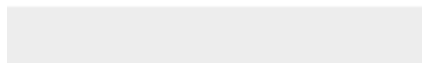


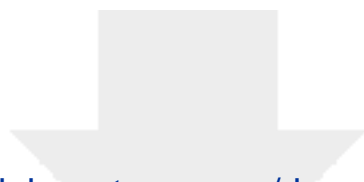


[Click here to access/download](#)

Supplemental code file (if applicable)

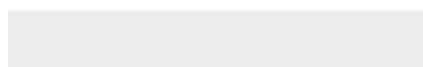
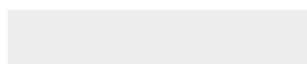
st001_cpv_index_good.mat

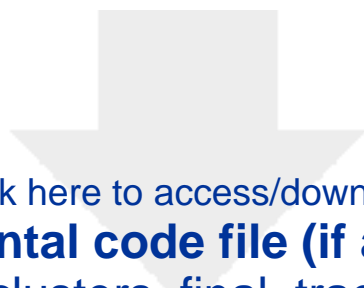




[Click here to access/download](#)

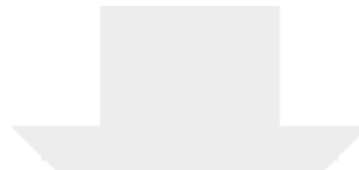
Supplemental code file (if applicable)
st001_clusters_final_matched.gdf





[Click here to access/download](#)

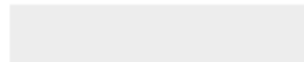
Supplemental code file (if applicable)
st001_clusters_final_tracked.gdf



[Click here to access/download](#)

Supplemental code file (if applicable)

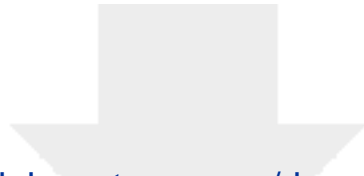
`calc_rotation.m`





[Click here to access/download](#)

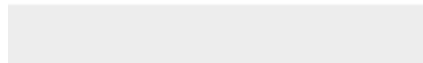
Supplemental code file (if applicable)
`splice_tracks.m`



[Click here to access/download](#)

Supplemental code file (if applicable)

`bc_sk_find_frame_colors.m`



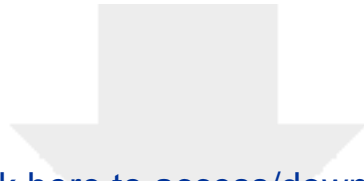


[Click here to access/download](#)

Supplemental code file (if applicable)

bc_sk_plot_model.m





[Click here to access/download](#)

Supplemental code file (if applicable)

bc_triad.m





[Click here to access/download](#)

Supplemental code file (if applicable)
README_videos.txt



[Click here to access/download](#)

Supplemental code file (if applicable)

bc_cross.m

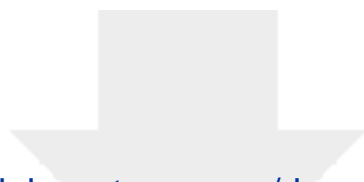




[Click here to access/download](#)

Supplemental code file (if applicable)
`bc_degenerateorientations_plots.m`

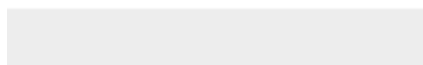
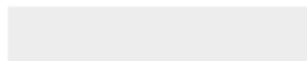


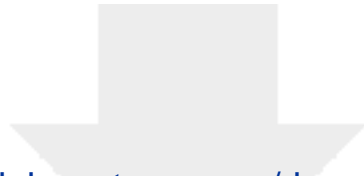


[Click here to access/download](#)

Supplemental code file (if applicable)

bc_jack.m



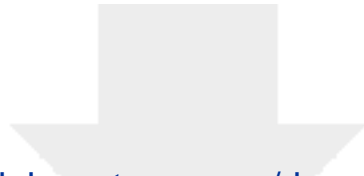


[Click here to access/download](#)

Supplemental code file (if applicable)

`bc_new_residual_plot.m`



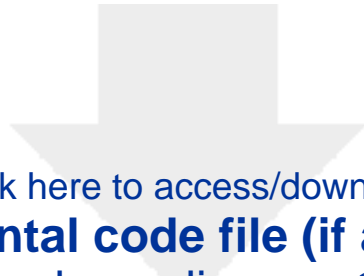


[Click here to access/download](#)

Supplemental code file (if applicable)

bc_sk_leastSqOriPos1.m





[Click here to access/download](#)

Supplemental code file (if applicable)

bc_sk_nonlinearopt.m





[Click here to access/download](#)

Supplemental code file (if applicable)

README_clust.txt





[Click here to access/download](#)

Supplemental code file (if applicable)
calibProj_Tsai.m

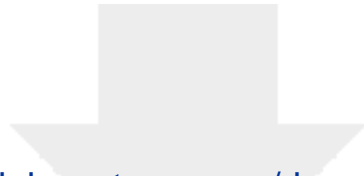




[Click here to access/download](#)

Supplemental code file (if applicable)
README_calib.txt





[Click here to access/download](#)

Supplemental code file (if applicable)

`find_orientation.m`





[Click here to access/download](#)

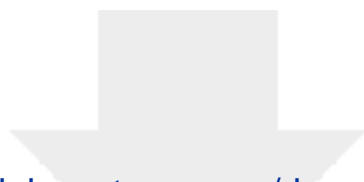
Supplemental code file (if applicable)
gg_ori.m





[Click here to access/download](#)

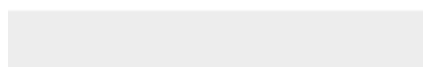
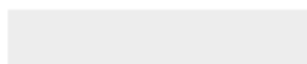
Supplemental code file (if applicable)
README_data.txt

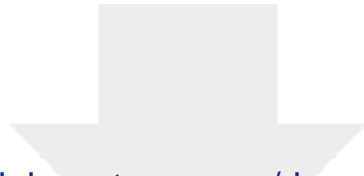


[Click here to access/download](#)

Supplemental code file (if applicable)

bc_euler.m

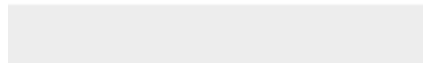


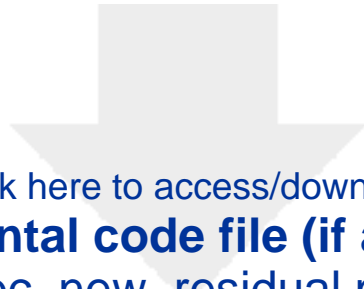


[Click here to access/download](#)

Supplemental code file (if applicable)

bc_min_rotation_finder.m





[Click here to access/download](#)

Supplemental code file (if applicable)

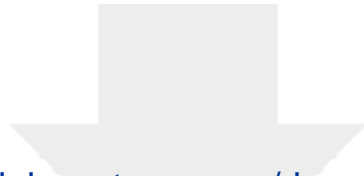
bc_new_residual.m



[Click here to access/download](#)

Supplemental code file (if applicable)
`bc_object.m`

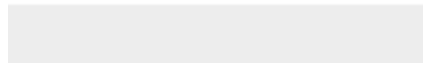


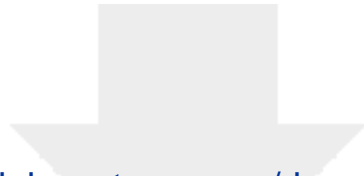


[Click here to access/download](#)

Supplemental code file (if applicable)

bc_sk_gaussian_intensity_multiple_rods.m





[Click here to access/download](#)

Supplemental code file (if applicable)

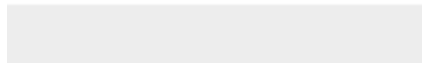
`bc_sk_leastSqOriPos.m`





[Click here to access/download](#)

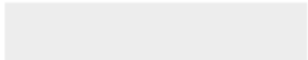
Supplemental code file (if applicable)
st001_spliced_modelresult.mat

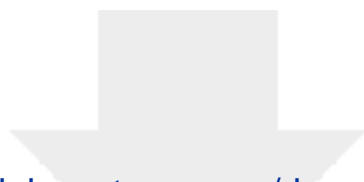




[Click here to access/download](#)

Supplemental code file (if applicable)
README_extra.txt

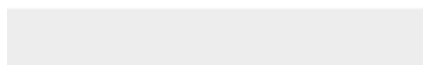
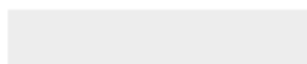




[Click here to access/download](#)

Supplemental code file (if applicable)

cpv_reader.m



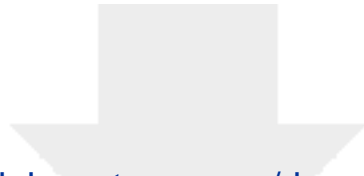


[Click here to access/download](#)

Supplemental code file (if applicable)

st001_fixed_modelresult.mat





[Click here to access/download](#)

Supplemental code file (if applicable)

st001_opt_modelresult.mat

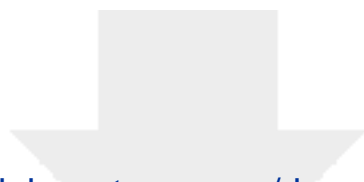




[Click here to access/download](#)

Supplemental code file (if applicable)
st001_fixed.mat

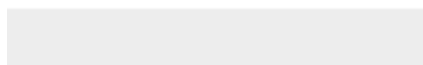
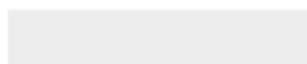




[Click here to access/download](#)

Supplemental code file (if applicable)

README_c1.txt



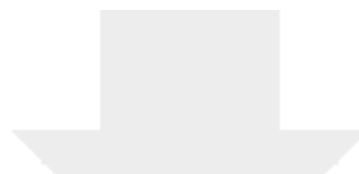


[Click here to access/download](#)

Supplemental code file (if applicable)

st001_c1.cpv

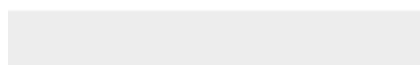
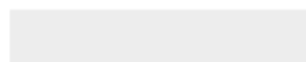


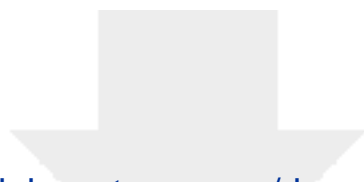


[Click here to access/download](#)

Supplemental code file (if applicable)

st001_c2.cpv

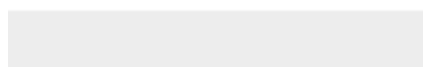
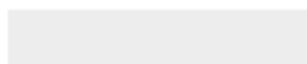




[Click here to access/download](#)

Supplemental code file (if applicable)

README_c2.txt

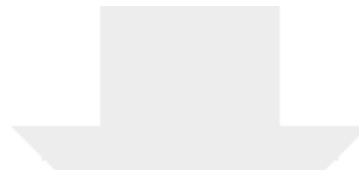




[Click here to access/download](#)

Supplemental code file (if applicable)
st001_c3.cpv

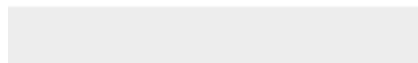
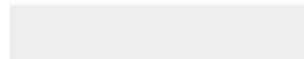


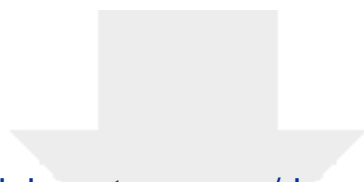


[Click here to access/download](#)

Supplemental code file (if applicable)

README_c3.txt

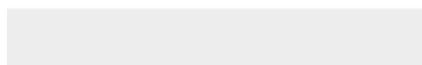
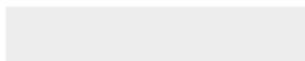




[Click here to access/download](#)

Supplemental code file (if applicable)

README_c4.txt





[Click here to access/download](#)

Supplemental code file (if applicable)
st001_c4.cpv

